

# **Experimental Investigation and Modelling of Heat Loss Mechanism from Offshore Buried Pipelines**

by

© Suvra Chakraborty

A thesis submitted to  
School of Graduate Studies  
in partial fulfilment of the  
requirements for the degree of  
Master of Engineering

Faculty of Engineering and Applied Science  
Memorial University of Newfoundland

**May 2017**

St John's

Newfoundland

to my family

# Abstract

Modeling of heat loss from offshore buried pipelines is one of the major concerns for oil and gas industries. Offshore oil and gas production and thermal modeling of buried pipelines in Arctic regions are challenging tasks due to the harsh environmental conditions and hazards. Heavy components of crude oil start to precipitate as wax crystal when the fluid temperature drops. Gas hydrates also form when natural gas combines with free water at high pressure and low temperature. Significant heat loss may occur from offshore buried pipelines in the forms of heat conduction and natural convection through the seabed. The later can become more prominent where the backfill soil is loose or sandy.

Theoretical shape factor model was widely utilized to estimate heat loss from buried pipelines. Several benchmark tests were performed to ensure the validity of the test using theoretical shape factor models which depend on the amount of heat flow, thermal conductivity and geometry of the surrounding medium.

The degree of saturation of surrounding medium can play a significant role in the thermal behavior of fluid traveling through the backfill soil. This research presents several steady state and transient response analysis describing some influential geotechnical parameters along with test procedures for different parameters such as burial depth, backfill soil, trench geometries, etc.

Several shutdown (cooldown) tests were performed to show the transient response in the dry and saturated sand medium. The outcomes of this research will provide valuable experimental data and numerical predictions for offshore pipeline design, heat loss from buried pipelines in offshore conditions, and efficient model to mitigate the flow assurance issues e.g. wax and hydrates.

## **Acknowledgements**

I would like to express my sincere gratitude and appreciation to all those who gave me their support, assistance and necessary advice to complete my research work and write this thesis.

Above all other, my sincere gratitude is extended to my supervisor Dr. Vandad Talimi for his appreciable support, helpful guidance, and encouragement throughout the entire master program. His detailed and constructive comments, patience and understanding helped me towards the successful completion of thesis work.

I would also like to express my gratitude to Dr. Yuri Muzychka, my co-supervisor, for his comments which made the research work more constructive.

Special thanks and appreciation are due to Dr. Rodney McAfee, Geotechnical Director at C-CORE and Mr. Gerry Piercey, Centrifuge Manager at C-CORE, who provided significant technical assistance with the testing program and publications. I greatly thank to Mr. Karl Kuehnemund, Mr. Derry Nicole, and Mr. Karl Tuff for their immense hard work to complete the test set up and continuous support during testing.

My heartfelt thanks go to Research & Development Corporation of Newfoundland and Labrador (RDC) for sponsoring the research.

Finally, I am thanking my family, for believing and encouraging me throughout my research work.

# Table of Contents

|                                               |    |
|-----------------------------------------------|----|
| 1 Introduction.....                           | 1  |
| 1.1 Background and Scope of Work .....        | 1  |
| 1.2 Objectives of the Research .....          | 4  |
| 1.3 Organization of the Thesis .....          | 4  |
| 2 Literature Review.....                      | 6  |
| 2.1 General Problem Definition .....          | 6  |
| 2.1.1 Backfill Effects on Heat Transfer.....  | 7  |
| 2.1.2 Pipeline Burial .....                   | 9  |
| 2.1.3 Porous Medium Thermal Conductivity..... | 10 |
| 2.2 Shape Factor and Other Models .....       | 10 |
| 2.3 Geotechnical Parameters: .....            | 14 |
| 2.3.1 Water Content, $w$ :.....               | 14 |
| 2.3.2 Degree of Saturation, $S_r$ : .....     | 15 |
| 2.3.3 Void Ratio, $e$ : .....                 | 15 |
| 2.3.4 Porosity, $n$ :.....                    | 15 |
| 2.3.5 Specific Volume, $v$ :.....             | 15 |
| 2.3.6 Air Content or Air Voids, $A$ :.....    | 16 |
| 2.3.7 Bulk Density, $\rho$ :.....             | 16 |
| 2.3.8 Specific Gravity, $G_s$ :.....          | 16 |

|                                                                   |    |
|-------------------------------------------------------------------|----|
| 2.4 Thermo-fluids Dimensionless Groups .....                      | 17 |
| 2.4.1 Reynolds number.....                                        | 17 |
| 2.4.2 Prandtl number .....                                        | 17 |
| 2.4.3 Biot number.....                                            | 18 |
| 2.4.4 Nusselt number.....                                         | 18 |
| 2.4.5 Rayleigh number .....                                       | 18 |
| 2.4.6 Grashof number .....                                        | 19 |
| 2.5 Convection Heat Transfer in Soil.....                         | 20 |
| 2.6 Effects of Degree of Saturation on Thermal Conductivity ..... | 22 |
| 2.7 Statistical and Uncertainty Analysis .....                    | 23 |
| 2.7.1 Shapiro- Wilk Test .....                                    | 23 |
| 2.7.2 Welch's t Test.....                                         | 24 |
| 2.7.3 Uncertainty Analysis .....                                  | 24 |
| 3 Experimental Analysis .....                                     | 26 |
| 3.1 Design of Experiment.....                                     | 26 |
| 3.1.1 Pipe Model .....                                            | 27 |
| 3.1.2 Soil Box and Soil Type .....                                | 29 |
| 3.1.3 Ice Water Containing Box .....                              | 31 |
| 3.1.4 Resistance Temperature Detectors (RTD's).....               | 33 |
| 3.1.5 Thermal Property Analyzer .....                             | 34 |

|                                                                  |    |
|------------------------------------------------------------------|----|
| 3.1.6 Temperature Control Panel and Data Acquisition System..... | 36 |
| 3.2 Benchmark Tests .....                                        | 37 |
| 3.3 Saturated Tests .....                                        | 38 |
| 3.3.1 Sample Saturation of Test Sand .....                       | 38 |
| 3.3.2 Saturated Tests .....                                      | 40 |
| 4 Results and Discussions.....                                   | 47 |
| 4.1 Benchmark Tests Result and Validation .....                  | 47 |
| 4.2 Saturated Tests Result .....                                 | 51 |
| 4.3 Saturated Tests Cooldown Curves .....                        | 54 |
| 5 Conclusions.....                                               | 59 |
| 5.1 Review of Important Observations .....                       | 59 |
| 5.2 Future Recommendations.....                                  | 61 |
| List of Publications from this Thesis .....                      | 62 |
| Bibliography .....                                               | 63 |
| Appendix A- Benchmark Tests Results .....                        | 67 |
| Appendix B- Saturated Tests Results .....                        | 75 |

# List of Figures

|                                                                                                                                          |    |
|------------------------------------------------------------------------------------------------------------------------------------------|----|
| Figure 1-1: A typical gas hydrate curve.....                                                                                             | 2  |
| Figure 1-2: Unsteady state process after pipeline shutdown. ....                                                                         | 3  |
| Figure 2-1: Heat transfer from a buried pipe into sea water. ....                                                                        | 6  |
| Figure 2-2: Grain size chart (Wentworth,1922).....                                                                                       | 8  |
| Figure 2-3: Buried pipe nomenclature. ....                                                                                               | 12 |
| Figure 2-4:The effective cylinder model (left) and the simplified buried pipeline definitions<br>(right), from Archer at al. (1997)..... | 13 |
| Figure 2-5: Approximating backfill effects (conduction) using the bi-polar coordinate system,<br>from Archer et al. (1997).....          | 14 |
| Figure 2-6: Effect on Thermal conductivity at various degree of Saturation (Case et al,1984)...                                          | 22 |
| Figure 3-1: Schematic diagram of the experimental setup. ....                                                                            | 26 |
| Figure 3-2: Cylindrical Cartridge Heater used in the experiment.....                                                                     | 28 |
| Figure 3-3: CAD drawing of the soil box. ....                                                                                            | 30 |
| Figure 3-4: Soil box filled with dry sand. ....                                                                                          | 31 |
| Figure 3-5: Ice-Water containing box.....                                                                                                | 33 |
| Figure 3-6: Resistance Temperature Detector. ....                                                                                        | 34 |
| Figure 3-7: KD2 Pro Thermal Property Analyzer. ....                                                                                      | 35 |
| Figure 3-8: Sample test to measure degree of saturation of test. ....                                                                    | 39 |
| Figure 3-9: Empty Soil box with RTD's positioned and coarser sand below Geotextile.....                                                  | 41 |
| Figure 3-10: Saturation of test sand. ....                                                                                               | 42 |
| Figure 3-11: Schematic diagram for uniform saturated sand test. ....                                                                     | 43 |
| Figure 3-12: Trenching in sand.....                                                                                                      | 44 |

|                                                                                                                             |    |
|-----------------------------------------------------------------------------------------------------------------------------|----|
| Figure 3-13: Pipe or heater placed in open trench. ....                                                                     | 45 |
| Figure 3-14: After backfilling the trench. ....                                                                             | 46 |
| Figure 4-1: Power vs. boundary temperature difference graph at different burial depths for<br>benchmark tests. ....         | 48 |
| Figure 4-2: Dimensionless shape factor comparison for different burial depths from benchmark<br>tests. ....                 | 49 |
| Figure 4-3: Cool down curves of pipe wall for burial depth of 5d from benchmark tests.....                                  | 50 |
| Figure 4-4: Power vs. pipe wall temperature curves for forward tests. ....                                                  | 51 |
| Figure 4-5: Power vs. pipe wall temperature curves for backward tests. ....                                                 | 52 |
| Figure 4-6: Power comparison between backfill test 1 (saturated) and analytical shape factor<br>model for $D/d=4.04$ . .... | 54 |
| Figure 4-7: Cool down curves of pipe wall for uniform test. ....                                                            | 55 |
| Figure 4-8: Cool down curves of pipe wall for open trench test. ....                                                        | 55 |
| Figure 4-9: Cooldown curves of pipe wall for backfill test 1 at burial depth, $D/d=4.04$ .....                              | 56 |
| Figure 4-10: Cooldown curves of pipe wall for backfill test 2 at burial depth, $D/d=4.46$ .....                             | 56 |
| Figure 4-11: Cooldown curves of pipe wall for backfill test 3 at burial depth, $D/d=4.04$ .....                             | 57 |
| Figure 4-12: Cooldown curves for different saturated tests.....                                                             | 58 |

## List of Tables

|                                                                                                                 |    |
|-----------------------------------------------------------------------------------------------------------------|----|
| Table 3-1: Cartridge Heater Specifications.....                                                                 | 28 |
| Table 3-2: Thermal boundary effects at different soil box dimensions compared to the shape<br>factor model..... | 30 |
| Table 3-3: Parameters obtained from sample saturated test. ....                                                 | 38 |
| Table 3-4: Parameters obtained from sample saturated test. ....                                                 | 40 |
| Table 3-5: Hydraulic Conductivity Coefficient Table.....                                                        | 41 |
| Table 3-6: Parameters obtained from uniform saturation test. ....                                               | 43 |

## List of Symbols and Abbreviations

|            |   |                                               |
|------------|---|-----------------------------------------------|
| A          | = | Air Content or Air Void                       |
| D          | = | Burial Depth, (mm)                            |
| K          | = | Permeability                                  |
| L          | = | Length of Pipe, (mm)                          |
| N          | = | Sample Size                                   |
| Q          | = | Power, (W)                                    |
| R          | = | Thermal Resistance                            |
| S          | = | Shape Factor, (m)                             |
| $\Delta T$ | = | Temperature Difference ( $^{\circ}\text{C}$ ) |
| V          | = | Total Volume of Soil                          |
| X          | = | Burial Depth(D)/Pipe Diameter(d)              |
| c          | = | Specific Heat Capacity (J/Kg-K)               |
| d          | = | Pipe Diameter (mm)                            |
| e          | = | Void Ratio                                    |
| h          | = | Latent Heat, (J/kg)                           |
| k          | = | Thermal Conductivity, (W/m-K)                 |
| n          | = | Porosity                                      |

|               |   |                                |
|---------------|---|--------------------------------|
| $q$           | = | Heat Flux, (W/m <sup>2</sup> ) |
| $r$           | = | Radius of the Pipe, (mm)       |
| $v$           | = | Specific Volume                |
| $w$           | = | Water Content                  |
| $\rho$        | = | Bulk Density of Soil           |
| $\mu$         | = | Viscosity of Fluid             |
| $\tilde{\mu}$ | = | Effective Viscosity            |
| $\alpha$      | = | Thermal Diffusivity            |
| $\beta$       | = | Fluid Expansion Coefficient    |
| $Bi$          | = | Biot Number                    |
| $D'$          | = | Equivalent Burial Depth        |
| $D_e$         | = | Equivalent Bed Diameter        |
| $\Phi$        | = | Porosity of the sand           |
| $C_p$         | = | Specific Heat Capacity         |
| $Gr$          | = | Grashof Number                 |
| $G_s$         | = | Specific Gravity               |
| $M_s$         | = | Mass of Soil                   |
| $M_w$         | = | Mass of Water                  |
| $Nu$          | = | Nusselt Number                 |

|                |   |                                                          |
|----------------|---|----------------------------------------------------------|
| $Pr$           | = | Prandlt Number                                           |
| $Q_L$          | = | Heat Flux thorough Pipe Wall per unit Length, (W/m)      |
| $Ra$           | = | Rayleigh Number                                          |
| $Re$           | = | Reynolds Number                                          |
| $S^*$          | = | Dimensionless Shape Factor                               |
| $Sr$           | = | Degree of Saturation                                     |
| $S_{u,invert}$ | = | Shear Strength at the Pipeline Invert                    |
| $T_o$          | = | Ambient Temperature of Medium, (K)                       |
| $T_p$          | = | Pipe Wall Temperature, (K)                               |
| $V_a$          | = | Volume of Air                                            |
| $V_s$          | = | Volume of Solids                                         |
| $V_v$          | = | Volume of Void                                           |
| $V_w$          | = | Volume of Water                                          |
| $V_{ult}$      | = | Vertical Pipe-Soil Force per unit Length of the Pipeline |
| $d_s$          | = | Sphere Diameter                                          |
| $h_b$          | = | Height of the Bed                                        |
| $k_b$          | = | Conduction Heat Transfer Coefficient of the Body         |
| $k_e$          | = | Effective Thermal Conductivity, (W/m-k)                  |
| $k_f$          | = | Thermal Conductivity of Fluid                            |

|           |   |                                 |
|-----------|---|---------------------------------|
| $k_s$     | = | Thermal Conductivity of Soil    |
| $k_{vp}$  | = | Plastic Stiffness               |
| $r_i$     | = | Pipe Radius, (m)                |
| $\vec{v}$ | = | Darcy Velocity                  |
| $w_b$     | = | Width of the Bed                |
| $w_d$     | = | Vertical Penetration            |
| $\rho_f$  | = | Fluid Density                   |
| $\rho_s$  | = | Particle Density                |
| $\rho_w$  | = | Water Density                   |
| ROV       | = | Remotely Operated Vehicle       |
| RTD       | = | Resistance Temperature Detector |

# Chapter 1

## 1 Introduction

### 1.1 Background and Scope of Work

The economy of many countries has experienced major turnarounds in recent years and most of which rely on the offshore and onshore oil sectors (Ewida et al, 2004). Due to significant discoveries of hydrocarbons in the Arctic region future production of Oil and Gas in that region will expand more in near future. Offshore oil and gas production in Arctic areas is challenging due to harsh environmental conditions. Thermal management of these assets is critical when the ambient temperature is low. Solid formation in the production path can have serious implications on production. The temperature of the soil-water system surrounding a submarine pipeline is usually much lower than the temperature of production fluids. The pipeline is constantly at risk of reaching low temperatures which may lead to critical problems such as excessive pressure loss due to phase changes and flow regime shifts, corrosion and erosion, wax build up, and hydrate formation which may lead to complete blockage of the pipeline (Sadegh et al, 1987). This significant temperature difference induces heat to flow from the oil to the environment. Heavy components of crude oil start to precipitate as wax crystal when the fluid temperature is low and the viscosity also increases upon a decrease in temperature which may block the pipelines. Gas hydrate also forms when natural gas combines with free water at high pressure and low temperature. For efficient transportation, it is necessary, therefore, that the crude be at a relatively high temperature so that it has a low viscosity. Passive insulation or active heating have been

used to mitigate these issues. In order to design these mitigation techniques, one should understand the complicated heat transfer mechanism through the saturated seabed backfill soil. Figure 1-1 is a typical gas hydrate curve which shows that if the working pressure is increased at a constant temperature (line A) or the temperature drops at a constant pressure (line B) the operational condition may fall into the hydrate region. The flow assurance analysis target is to keep the working condition in the "Non-Hydrate Region" or shifting the hydrate curve to the left (Guo et al, 2005).

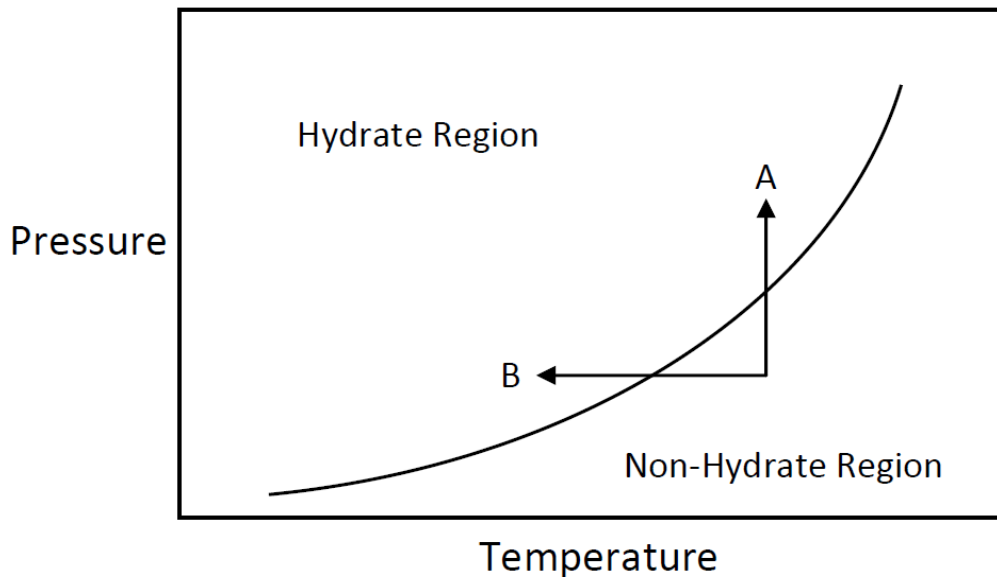


**Figure 1-1: A typical gas hydrate curve.**

Several studies reported that heat loss from buried pipelines to surrounding medium is mainly due to the heat conduction. But recent studies show that, based on soil conditions heat loss from buried pipelines through natural convection can be significant due to water circulation in the sea bed soil. The type of seabed soil can vary from clay to gravel. Furthermore, the soil will be disturbed and become loose through the process of trenching and backfilling, which further increases the chance of natural convection. Pipeline thermal

response after shutdown (i.e. known as cool down time) is another important phenomenon to consider during operation of buried pipelines. Figure 1-2 illustrates a typical pipeline temperature history after the shutdown. The temperature should not fall below the critical temperature to prevent hydrate formation. The No Touch time is very important for the operators, and if it is long enough, it provides a good opportunity for the operator to find and fix the issue without executing additional procedures to prevent formation of hydrates. The no touch time can be increased providing extra insulation but it will increase the capital expenditure. Thermodynamic inhibitors such as methanol or mono ethelene glycol (MEG) can also be used to shift the hydrate curve towards the left, preventing the pipeline from becoming blocked.

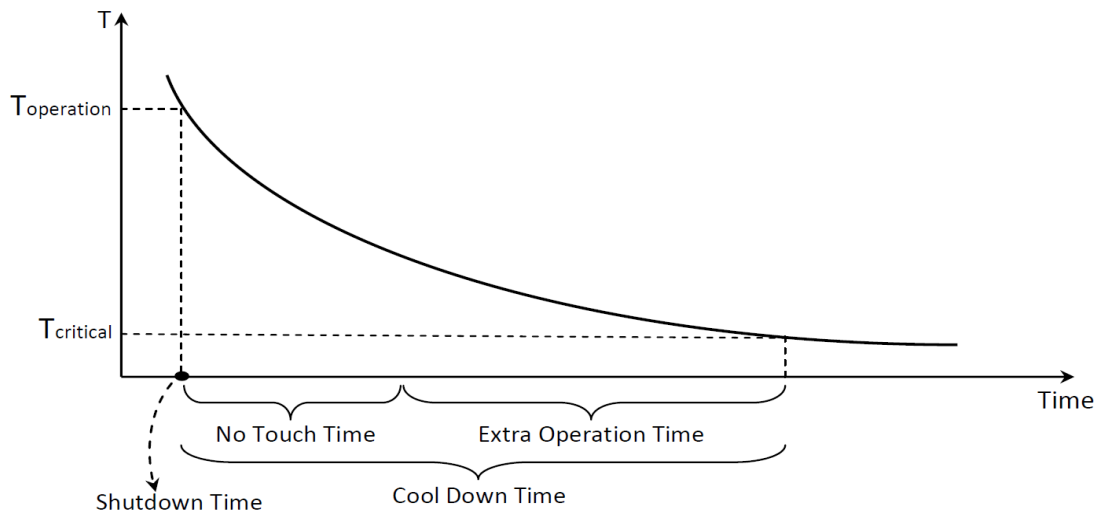


**Figure 1-2: Unsteady state process after pipeline shutdown.**

## 1.2 Objectives of the Research

The research work is mainly based on experimental analysis. Though some early stage numerical analysis were performed with dry sand medium to validate the experimental model along with theoretical models. The objectives of this thesis work can be described as follows:

- Design of experiment and validation of the experimental process with theoretical proposed model to calculate heat loss from offshore buried pipeline;
- Provide an insight of the heat loss phenomena from buried pipeline in offshore conditions using experimental results;
- Conducting several tests with different parameters describing some geotechnical parameters;
- Performing several cooldown (shutdown) tests to capture the transient behaviour of the buried pipeline; and
- Provide suggestions for future research based on the observations of the present work and discuss the limitations of the present research.

## 1.3 Organization of the Thesis

- **Chapter 1:** The first chapter addresses the background and aim of the proposed research. The desired outcome of the research explained here briefly.
- **Chapter 2:** This chapter covers a literature review related to modelling of heat loss from offshore buried pipelines, discuss several geotechnical and heat transfer parameters and uncertainty analysis.

- **Chapter 3:** Design of experiments with detailed explanation of methodology to perform the tests are presented in this chapter.
- **Chapter 4:** This chapter illustrates the outcomes of the research for different parameters along with discussion and conclusions.
- **Chapter 5:** This chapter summarizes the major findings, conclusion of work, and possible future recommendations to continue the research.

# Chapter 2

## 2 Literature Review

### 2.1 General Problem Definition

Different modes of heat transfer from a typical offshore buried pipeline are shown in Figure 2-1. Heat loss through conduction has been assumed the most prominent mode of heat transfer among them (Barletta et al, 2008). High porosity and permeability of the backfill soil with a very loose state compared to original undisturbed soil, can lead to an increase in natural heat convection around the buried pipeline (Atwan et al, 2005). Grain size is one of the important soil parameters

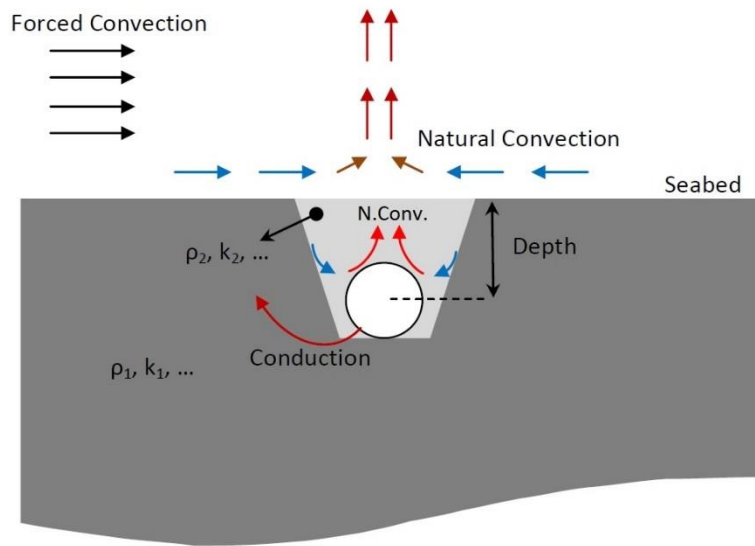


**Figure 2-1: Heat transfer from a buried pipe into sea water.**

that significantly affects permeability and convection heat transfer (natural and forced) in porous media. Different grain size is expected in varying offshore locations from sand to clay. Most of

the existing heat transfer models are limited to a special soil material. For example, Atwan and Sakr (2005) studied heat transfer from a buried horizontal cylinder in saturated soil using both numerical and experimental methods. The sand grain size in their study is 2.7 (mm) which is considered as a large size. They showed that therefore, there is a need for heat transfer models for a range of possible seabed soil properties for offshore oil and gas projects.

### **2.1.1 Backfill Effects on Heat Transfer**

During the trenching and backfill process for offshore pipelines, soil properties change due to change in the water saturation level. Therefore, the backfill soil does not have same density, conductivity, etc. as the original soil. The soil thermal conductivity depends on grain-size distribution, dry density, moisture content, and mineral composition (Wintehkorn et al, 1960). In the existing heat transfer models including the shape factors, the soil properties around the pipe have been assumed uniform. Vollaro et al. (2011) is one of the rare numerical studies considering different backfill soil properties. Based on the nature of their study i.e. onshore, they only solved heat conduction in the soil, and the effects of heat convection have been neglected. Furthermore, a constant soil surface temperature has been assumed, that is not applicable to offshore applications due to the effects of natural and forced convections in the sea water. Zakarian et al. (2012) studied heat transfer from partially and fully buried offshore pipelines, but they assumed uniform soil properties and a fixed convection heat transfer coefficient on the surface which are limitations of their study. The heat conduction coefficient also changes during the trench and backfill process. The soil thermal conductivity is usually a function of different parameters such as saturation level, dry density, temperature, moisture content, grain size/shape, mineralogy, and volumetric ratios of solid, liquid, and gas phases. The soil properties change

significantly during the trenching and backfill process. Compare to the original soil, the backfill soil is in a very loose state due to the increase in water content and other effects. The backfill soil usually possesses high porosity and permeability leading to an increase in natural heat convection around the buried pipe.

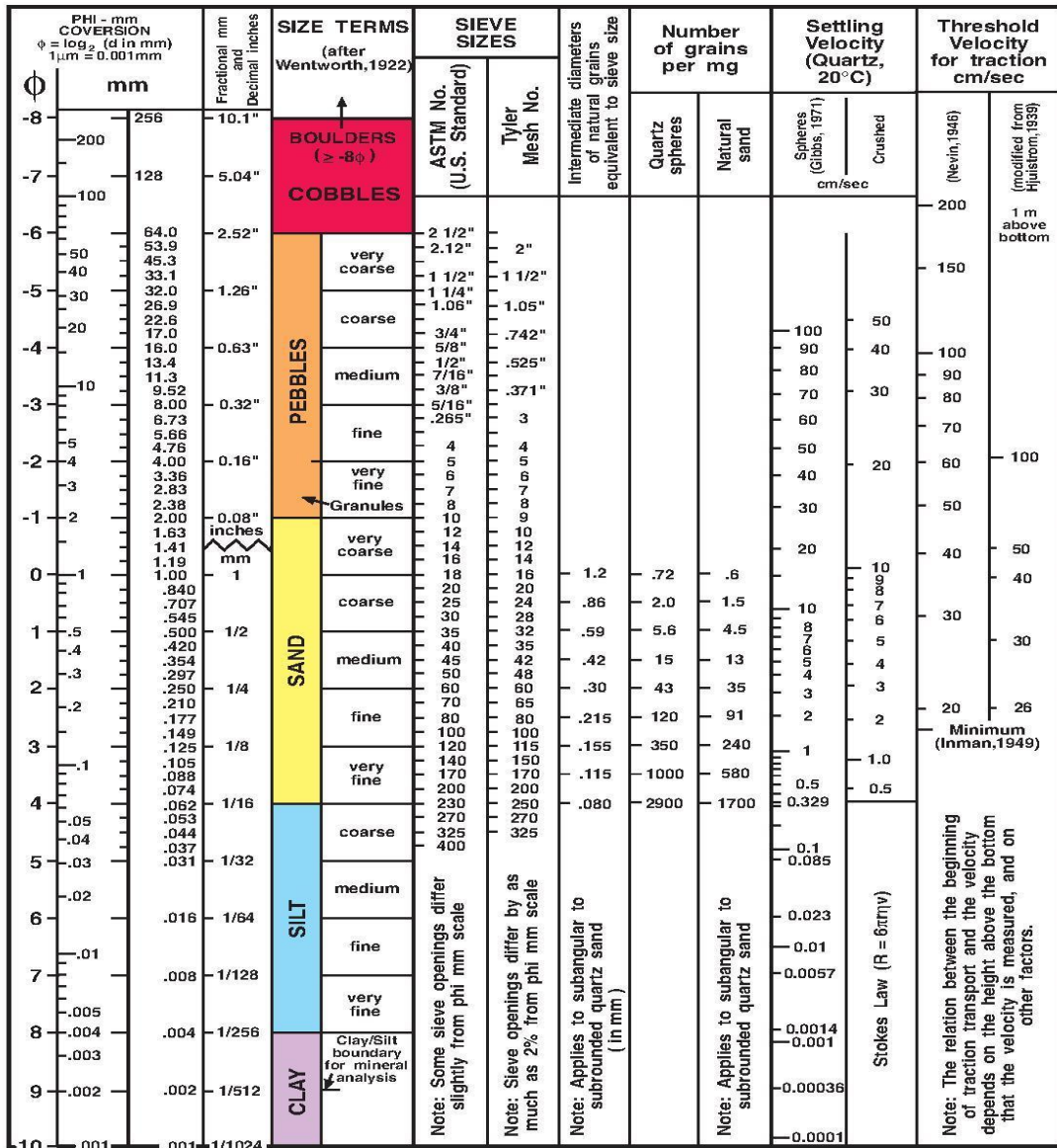


Figure 2-2: Grain size chart (Wentworth, 1922)

## 2.1.2 Pipeline Burial

Pipeline burial and trenching in some offshore developments are now one of the prime methods to avoid ice gouge, icebergs, and other threats. Pipeline trenching has been traditionally performed using jetting, but other methods such as mechanical ploughing and cutting has also been used in recent years. Selecting a trench technique depends on the sea bed and geotechnical conditions which should be assessed before the design process. In general, pipeline trenching can be performed before or after pipe laying.

In the jetting method, a high-pressure water flow generated in nozzles expels the soil. The nozzles are placed beneath the sea bed. Jetting systems may be mounted on Remotely Operated Vehicles (ROVs) or separate machines towed by vessels. Vessels may also tow large ploughs, another method of trenching, to create a buried pipeline route. The plough systems usually have skids in front and rear of them, cutting the soil and push it upward. These systems also include guides to lift a pre-laid pipeline if necessary. The third trenching method involves mechanical cutters. The cutting machines are often able to create trenches with different cross section shapes by controlling the position of their multiple rotating cutting blades. These three methods can also be used combined.

After laying the pipeline in the trench, a vertical penetration might happen depending on the pipe relative density and soil properties. For permeable soils, the vertical penetration can be estimated as:

$$\frac{w_d}{d} = \frac{V_{ult}/d}{k_{vp}} \quad (2.1)$$

where  $w_d$  is the vertical penetration,  $d$  is the pipeline diameter,  $V_{ult}$  is the vertical pipe-soil force

per unit length of the pipeline, and  $k_{vp}$  is the plastic stiffness.

$$\frac{V_{ult}}{S_{u,invert} d} = 6 \left( \frac{W}{d} \right)^{0.25} \quad (2.2)$$

where  $S_{u,invert}$  is the shear strength at the pipeline invert (Randolph et al, 2011).

### 2.1.3 Porous Medium Thermal Conductivity

The heat conduction through a porous medium occurs in two parallel paths: through the soil grains and through the fluid filled the pores. Thermal conductivity of the porous medium can be defined as:

$$k = \Phi k_f + (1 - \Phi) k_s \quad (2.3)$$

where  $\Phi$  is the porosity,  $k_f$  is the thermal conductivity of the fluid, and  $k_s$  is the thermal conductivity of the soil. This can be shown by integrating the energy conservation over a control volume of a homogeneous porous medium (Bejan,2013).

## 2.2 Shape Factor and Other Models

There are several models developed to represent the heat transfer from a buried pipeline. A classic approach is the two-dimensional heat transfer analysis using a Shape Factor model:

$$Q = k S \Delta T_{overall} \quad (2.4)$$

Where “S”, the Shape Factor is:

$$S = \frac{1}{k * R} \quad (2.5)$$

This model holds the following assumptions:

- Long pipe, so the problem can be assumed two dimensional
- Uniform soil properties around the buried pipe
- Isothermal pipe outer surface and soil surface

At present, there is no general formula available for predicting the stationary conduction shape factor for complex system. For simple component shapes and isothermal heat conduction shape factors for infinitely long hollow cylinder, flat plate, hollow spheres can be used. To determine the shape factor for complex geometry it is necessary to recognize a coordinate system appropriate for the geometry. Assuming the isothermal boundary condition, the temperature distributions can be obtained and local heat flux can also be calculated from the temperature distribution. The thermal resistance of the of the component is obtained from the definition of thermal resistance: total temperature drop across the component divided by the total heat flow rate. Estimating all the parameters with conduction shape factor thermal conductivity can be derived from Equation (2.4).

The shape factor,  $S$ , for a buried pipe can be determined using the following model (Hahne and Grigull, 1975):

$$S = \begin{cases} \frac{2\pi L}{\cosh^{-1}(D/r)} & L \gg r \\ \frac{2\pi L}{\ln(2D/r)} & L \gg r \text{ and } D > 3r \\ \frac{2\pi L}{\ln \frac{L}{r} \left[ 1 - \frac{\ln(L/2D)}{\ln(L/r)} \right]} & D \gg r \text{ and } L \gg D \end{cases} \quad (2.6)$$

where  $D$  is the burial depth to the pipe centerline,  $L$  is pipe length (i.e. unit in most thermal analysis), and  $r$  is the pipe radius, as shown in Figure 2-3.

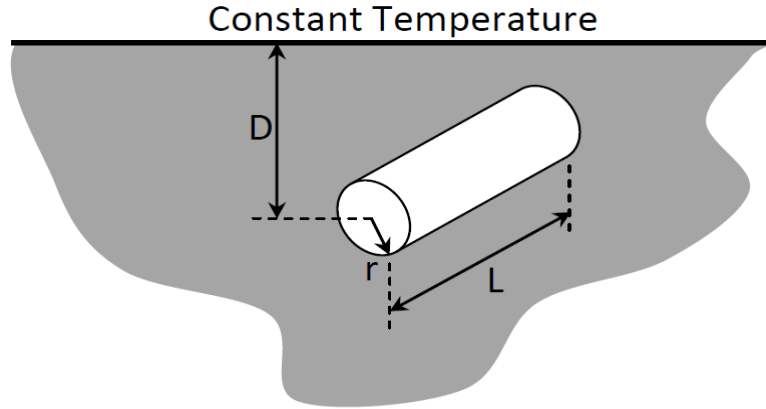


**Figure 2-3: Buried pipe nomenclature.**

As the power requirements and temperature difference are known from experimental analysis, Equation (2.4) has been used to calculate the experimental shape factor and compare those with the model proposed by Hahne and Grigull, 1975 (i.e. Equation (2.6) in the present study). Thiagarajan and Yovanovich, 1974 also proposed a model with constant flux boundary condition for thermal resistance (Equation 2.7) which can be used in conjunction with Equation (2.5) to calculate the shape factor as well.

$$R = \frac{\eta_0}{2\pi k} + \frac{1}{\pi k} \sum_{n=1}^{\infty} \frac{e^{-2n\eta_0}}{n} \tanh(n\eta_0) \quad (2.7)$$

Where,

$$\eta_0 = \cosh^{-1} \left( \frac{D}{r} \right) \quad (2.8)$$

Different models have been suggested for effective radius. If the soil surface is at a uniform convection boundary condition,  $h$ , the shape factor can be approximately calculated using Eq. (2.6). with an equivalent burial depth calculated as follows (Schneider, 1973):

$$D' = D + \frac{k}{h} \quad (2.9)$$

Archer and O'Sullivan,1997 developed two models (i.e. the effective cylinder model where the burial medium is approximated by an annular region and a half space model that contains a more realistic region with the pipe located at its real depth). Effective cylinder model calculates effective diameter based on pipe diameter, burial depth, and Biot number. Non-homogeneous half space is common for buried heat transfer analysis. The thermal properties of soils are important in a variety of applications, including the thermal performance of buried pipelines and geothermal heat pumps. For a half space model and using the Bau and Sadhai (1982) approximation, they expressed the average heat flux per unit pipe surface area,  $q$  by the following equation:

$$q = \frac{Q_L}{2\pi r_i} = \frac{Sk_e(T_p - T_o)}{r_i} \quad (2.10)$$

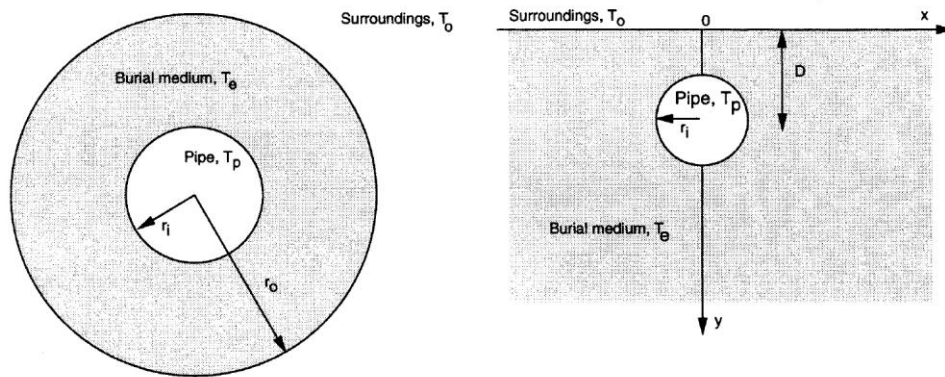


**Figure 2-4: The effective cylinder model (left) and the simplified buried pipeline definitions (right), from Archer et al. (1997).**

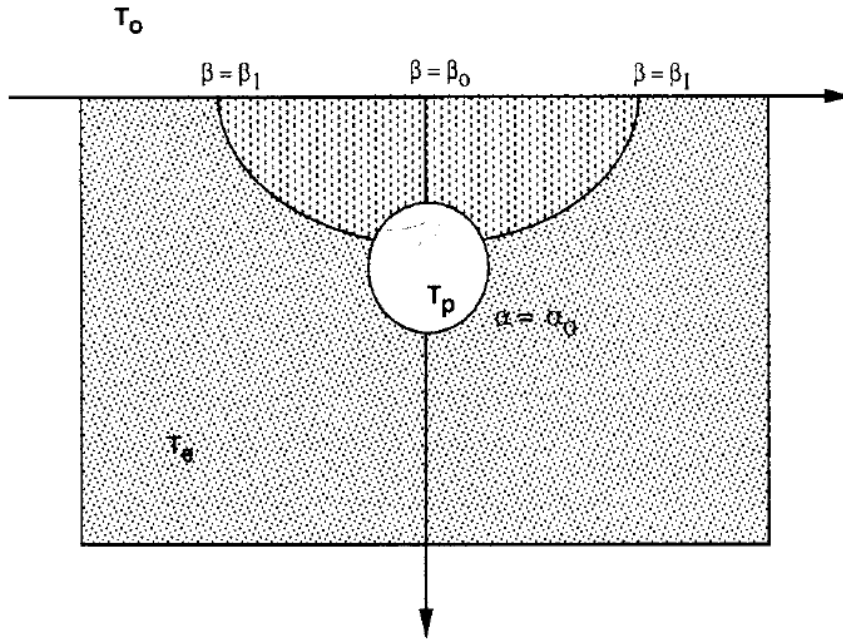


Figure 2-5: Approximating backfill effects (conduction) using the bi-polar coordinate system, from Archer et al. (1997).

## 2.3 Geotechnical Parameters:

It is important to know about the influential geotechnical parameters (Craig,2013) and their effect on the heat loss mechanism in order to design the experimental setup efficiently.

### 2.3.1 Water Content, w:

The water content is determined by weighing a sample of the soil and then drying the sample in an oven at a temperature of 105-110°C and reweighing. Drying period should be normally 24 hours.

$$w = \frac{M_w}{M_s} \quad (2.11)$$

### **2.3.2 Degree of Saturation, $S_r$ :**

It is the ratio of volume of water to the volume of void space. The degree of saturation can range between zero for a completely dry soil to 1(100%) for a fully saturated soil.

$$S_r = \frac{V_w}{V_v} \quad (2.12)$$

### **2.3.3 Void Ratio, $e$ :**

The void ratio,  $e$  is the ratio of the volume of voids to the total volume of solids i.e.:

$$e = \frac{V_v}{V_s} \quad (2.13)$$

### **2.3.4 Porosity, $n$ :**

It is the ratio of volume of voids to the total volume of the soil, i.e.:

$$n = \frac{V_v}{V} \quad (2.14)$$

The void ratio and the porosity are inter-related as follows:

$$e = \frac{n}{1 - n} \quad (2.15)$$

$$n = \frac{e}{1 + e} \quad (2.16)$$

### **2.3.5 Specific Volume, $v$ :**

It is the total volume of soil which contains unit volume of solids, i.e.

$$v = 1 + e \quad (2.17)$$

### 2.3.6 Air Content or Air Voids, A:

Air voids is the ratio of the volume of air to the total volume of soil, i.e.

$$A = \frac{V_a}{V} \quad (2.18)$$

### 2.3.7 Bulk Density, $\rho$ :

The bulk density of a soil is the ratio of the total mass to the total volume i.e.:

$$\rho = \frac{M}{V} \quad (2.19)$$

### 2.3.8 Specific Gravity, $G_s$ :

The specific gravity of soil particles ( $G_s$ ) is given by:

$$G_s = \frac{M_s}{V_s \rho_w} = \frac{\rho_s}{\rho_w} \quad (2.20)$$

Here,  $\rho_w$  is the density of water and  $\rho_s$  is the particle density.  $G_s$  is a dimensionless number and several expressions can be derived using that.

If the volume of solids is 1 unit then the volume of voids is  $e$  units. The mass of solids is then  $G_s \rho_w$  and from water content, the mass of water is  $w G_s \rho_w$ . So, the degree of saturation can be expressed as:

$$s_r = \frac{wG_s}{e} \quad (2.21)$$

The bulk density of soil can be expressed as:

$$\rho = \frac{G_s(1 + w)}{1 + e} \rho_w \quad (2.22)$$

Using Equation (2.21), Equation (2.22) can be rearranged as:

$$\rho = \frac{G_s + s_r e}{1 + e} \rho_w \quad (2.23)$$

## 2.4 Thermo-fluids Dimensionless Groups

### 2.4.1 Reynolds number

The Reynolds number,  $Re$ , is traditionally defined as:

$$Re = \frac{\rho UL}{\mu} \quad (2.24)$$

and represents the ratio between inertial and shear stress forces. In the equation above  $\rho$  is fluid density,  $U$  is velocity,  $L$  is a characteristic length, and  $\mu$  is fluid viscosity. Reynolds number is mostly used to determine whether a flow is laminar or turbulent.

### 2.4.2 Prandtl number

The Prandtl number,  $Pr$ , is defined as follows:

$$Pr = \frac{U}{\alpha} = \frac{\mu C_p}{k} \quad (2.25)$$

and is the rate of momentum diffusion versus the rate of thermal diffusion. In the equation above,  $\nu$  is momentum diffusion,  $\alpha$  is thermal diffusion,  $c_p$  is the specific heat capacity, and  $k$  is the thermal conductivity.

### 2.4.3 Biot number

The Biot number,  $Bi$ , is defined as follows:

$$Bi = \frac{hL}{k_b} \quad (2.26)$$

and provides a ratio of the thermal resistance inside and at the surface of a body. In the equation above,  $h$  is the convective heat transfer coefficient at the surface,  $L$  is a characteristic length, and  $k_b$  is the thermal conductivity of the body.

### 2.4.4 Nusselt number

The Nusselt number  $Nu$ , is defined as:

$$Nu = \frac{hL}{k} = \frac{qL}{k(T_s - T_\infty)} \quad (2.27)$$

and is a dimensionless heat transfer rate, defined based on the difference between surface temperature,  $T_s$ , and ambient temperature,  $T_\infty$ , for external flows. In the equation above,  $h$  is convective heat transfer coefficient,  $k$  is the thermal conductivity of the fluid, and  $q$  is heat flux.

### 2.4.5 Rayleigh number

The Rayleigh number,  $Ra$ , is defined as follows:

$$Ra = \frac{g\beta\Delta TL^3}{\alpha\nu} \quad (2.28)$$

and represents the strength of buoyancy forces. When Rayleigh number is low, the conduction is the dominant heat transfer mode. At high Rayleigh numbers, the heat transfer is mostly in the form of convection. When natural convection in porous media is of interest, a Darcy-modified Rayleigh number is used:

$$Ra = \frac{Kg\beta\Delta TL}{\alpha\nu} \quad (2.29)$$

In the equations above, K is the porous medium permeability, g is gravitational acceleration, and  $\beta$  is fluid's volume expansion coefficient at constant pressure:

$$\beta = -\frac{1}{\rho} \left( \frac{\partial \rho}{\partial T} \right)_p \quad (2.30)$$

If the fluid is not necessarily an ideal gas, density decreases slightly with an increase in the absolute temperature. This can be modeled using a first order Taylor series expansion as follows:

$$\rho \cong \rho_\infty [1 - \beta(T - T_\infty) + \dots] \quad (2.31)$$

## 2.4.6 Grashof number

The Grashof number, Gr, is defined as:

$$Gr = \frac{g\beta\Delta TL^3}{\nu^2} = \frac{Ra}{Pr} \quad (2.32)$$

and represents the ratio between buoyancy forces and viscous forces. Grashof number is used to determine whether a flow in a natural convection process is laminar or turbulent. Natural flows with low Grashof numbers are laminar, and at high Grashof numbers the flow is turbulent.

## 2.5 Convection Heat Transfer in Soil

After the burying process, the backfill soil properties do not match the native properties. Hydraulic conductivity, or permeability, increases significantly after the trenching and backfilling process. This will cause even more heat loss from buried pipe through natural convection heat transfer in the soil. A porous medium is a solid structure with voids which are internally connected and make random shaped passes through the solid material. The volume fraction of the porous material that is occupied by void space is called porosity,  $\Phi$ . Therefore,  $1 - \Phi$  is the volume fraction that is occupied by solid. Having defined the porosity, the continuity equation (mass conservation) for a control volume is:

$$\Phi \frac{\partial \rho_f}{\partial t} + \nabla \cdot (\rho_f \vec{v}) = 0 \quad (2.33)$$

where  $\rho_f$  is fluid density, and  $\vec{v}$  is Darcy velocity i.e. average of fluid velocity over total volume.

In modeling fluid dynamics in porous media, the momentum equation is replaced by Darcy law.

The Darcy law in vector form is:

$$\vec{v} = \frac{K}{\mu} (-\nabla P + \rho \vec{g}) \quad (2.34)$$

where  $K$  is an empirical constant called permeability.  $\sqrt{K}$  is a length scale that represents the effective pore diameter and can be used to define the Reynolds number as follows:

$$\text{Re} = \frac{u\sqrt{K}}{\nu} \quad (2.35)$$

The Darcy law assumes that the local Reynolds number does not exceed the range 1-10. Greater Reynolds numbers lead to non-linear drag where the form drag caused by hitting solid obstacles is comparable to friction due to surface. For this Reynolds number range Dupuit (1863) and Forchheimer (1901) suggested the following equation (known as Forchheimer's equation):

$$\nabla P = -\frac{\mu}{K}\mathbf{v} - \frac{c_F}{\sqrt{K}}\rho_f|\mathbf{v}|\mathbf{v} \quad (2.36)$$

$c_F$  is defined as:

$$c_F = 0.55 \left( 1 - 5.5 \frac{d_s}{D_e} \right) \quad (2.37)$$

where  $d_s$  is the sphere diameter and  $D_e$  is the equivalent bed diameter as follows:

$$D_e = \frac{2w_b h}{w_b + h} \quad (2.38)$$

and  $w_b$  and  $h_b$  are width and height of the bed, respectively.

There is another alternate to Darcy's equation known as Brinkman's equation:

$$\nabla P = -\frac{\mu}{K}\mathbf{v} + \tilde{\mu}\nabla^2\mathbf{v} \quad (2.39)$$

The equation above has also been referred to as "Brinkman's extension of Darcy's law" (Rubinstein, 1986). There are two viscous terms in the Brinkman's equation, the first one is the

Darcy viscous term, and the second one is analogous to non-linear term in Navier-Stokes equation.  $\tilde{\mu}$  is an effective viscosity (Nield and Bejan, 1999).

## 2.6 Effects of Degree of Saturation on Thermal Conductivity

Prior studies described that thermal conductivity and hydraulic conductivity increases sharply up to approximately 70% of degree of saturation. Figure 2-6 shows field measurements of thermal conductivity obtained by Cass et al. (1984) for unconsolidated soil at various moisture contents. The values at low water saturations appear to have a slope distinctly different from the slope seen at higher water saturations. However, several previous studies also reported that under

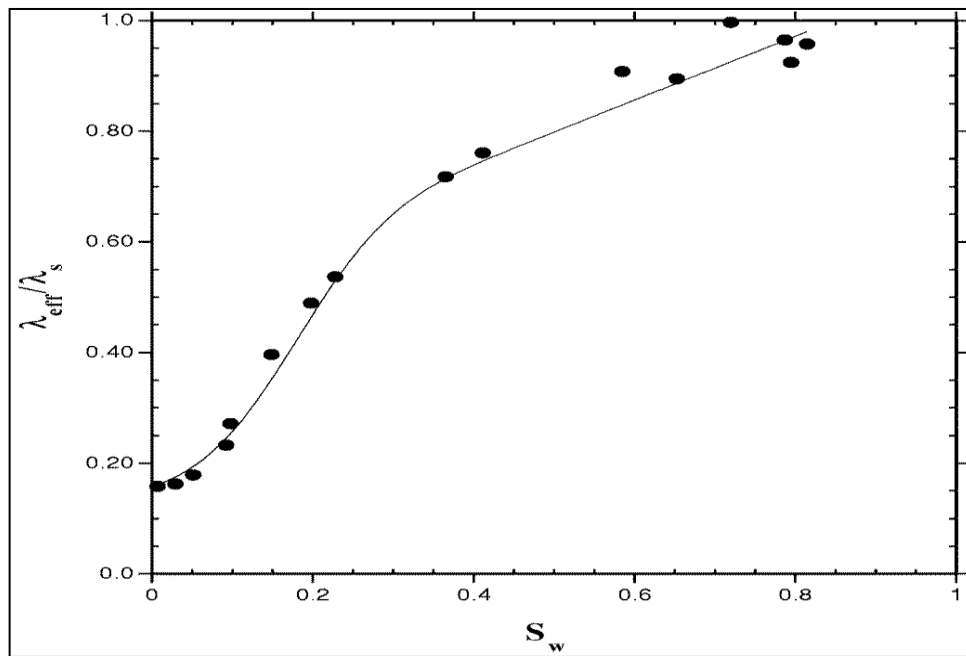


Figure 2-6: Effect on Thermal conductivity at various degree of Saturation (Case et al,1984).

atmospheric pressure the degree of saturation may be increased by displacing air in sand with  $CO_2$ , slow permeation from the base up, de-airing water before introducing into sand, and

passing a number of pore volumes of water through the sample. Therefore, the sand used for this research was saturated under atmospheric pressure.

## 2.7 Statistical and Uncertainty Analysis

### 2.7.1 Shapiro- Wilk Test

Shapiro-Wilk test is a test for the checking the normal distribution of the data. It works with the null hypothesis principle to check whether a sample came from normally distributed population or not (Royston, 1992).

The test statistic is defined as:

$$W = \frac{(\sum_{i=1}^n a_i x_i)^2}{\sum_{i=1}^n (x_i - \bar{x})^2} \quad (2.40)$$

Where,

$x_i$  is the value of the sample for corresponding  $i^{\text{th}}$  order.

$\bar{x}$  is the sample mean

$$a_1, \dots, a_n = \frac{m^T V^{-1}}{(m^T V^{-1} V^{-1} m)^{\frac{1}{2}}} \quad (2.41)$$

Where,

$$m = (m_1 \dots \dots m_n)^T \quad (2.42)$$

$m_1 \dots \dots m_n$  are the expected values of independent and randomly distributed identical random variables sampled from normal distribution and V is the covariance matrix of those order of statistics.

## 2.7.2 Welch's t Test

Welch's t-test is a statistical tool to check the statistical stability of the output. Welch's t-test is often referred to as unequal variances t-test as it assumes the normal distribution of the data and unequal variances (Johnson and Wichern,1992). For this research the null hypothesis was checked with Welch's t-test and t value in Welch's test is defined as:

$$t = \frac{\bar{Y}_1 - \bar{Y}_2}{\sqrt{\frac{s_1^2}{N_1} + \frac{s_2^2}{N_2}}} \quad (2.43)$$

Where,  $\bar{Y}_1$  and  $\bar{Y}_2$  are the sample means,  $s_1^2$  and  $s_2^2$  are the sample variances,  $N_1$  and  $N_2$  are the sample sizes of analytical and experimental outputs. The degree of freedom associated with the analysis can be estimated using the following equation:

$$v \approx \frac{\left(\frac{s_1^2}{N_1} + \frac{s_2^2}{N_2}\right)^2}{\frac{s_1^4}{N_1^2 * v_1} + \frac{s_2^4}{N_2^2 * v_2}} \quad (2.44)$$

## 2.7.3 Uncertainty Analysis

The uncertainty analysis for an experimental setup gives an overview to estimate the overall performance of the setup and suitability of the outputs (Holman,1966).

Equation (2.45) represents the governing equation to measure the shape factor.

$$S = \frac{Q}{k * \Delta T} \quad (2.45)$$

Uncertainty for the experimental outputs can be calculated using Equation (2.46).

$$w_s = S * \left[ \left( \frac{a_Q * w_Q}{Q} \right)^2 + \left( \frac{a_k * w_k}{k} \right)^2 + \left( \frac{a_{\Delta T} * w_{\Delta T}}{\Delta T} \right)^2 \right]^{\frac{1}{2}} \quad (2.46)$$

Here,  $w$  is the associated uncertainty. Comparing with Equation (2.45) the following parameters can be obtained.

$$a_Q = 1; a_k = -1; a_{\Delta T} = -1$$

The associated uncertainty with  $\Delta T$  can be expressed generally as:

$$w_{\Delta T} = \left[ \sum (a_i * w_{T_i})^2 \right]^{1/2} \quad (2.47)$$

Here,

$$\Delta T = T_1 - T_2;$$

$$a_1 = \frac{\delta \Delta T}{\delta T_1} \text{ and } a_2 = \frac{\delta \Delta T}{\delta T_2} \quad (2.48)$$

The accuracy of the devices used in the experiments were taken from user manuals and accuracy of temperature measurement was taken from calibration data of the RTDs to measure the overall uncertainty.

# Chapter 3

## 3 Experimental Analysis

### 3.1 Design of Experiment

The testing program includes several steps and design of experiment is one of the important aspects of this thesis. Figure 3-1 shows the schematic diagram of the experimental setup. A cylindrical cartridge heater was utilized as the pipe model in these experiments to model the warm buried pipeline. The temperature of the heater can be adjusted using control panel. The

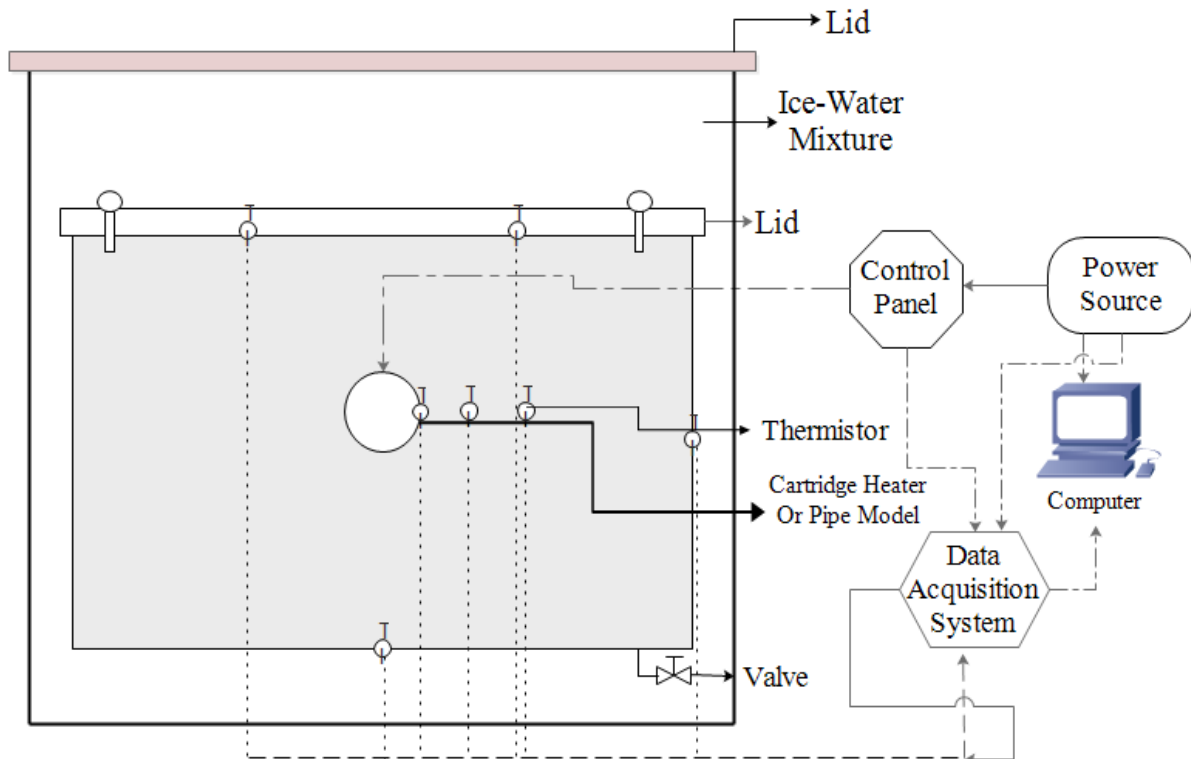


Figure 3-1: Schematic diagram of the experimental setup.

sand and the heater were placed in a test box, referred to hereon as soil box. The experimental setup required the boundary temperature to be close to 0°C, to match the ambient temperature presumed in seabed environment. The easiest way to achieve this thermal boundary condition was to insert the soil box inside a larger box and fill the space between the walls and bottoms with an ice-water mixture. This larger box is referred to as ice-water containing box. All the temperatures sensed by several thermistors placed at different locations and current passing through the heater was recorded using a data acquisition system.

The initial challenge for this research was to design and fabricate the experimental setup due to the large number of parameters involved in modeling the experiment. The main challenges to address before proceeding with the benchmark tests were as follows:

- Design of the soil box that would eliminate the boundary effects and hold vacuum pressure during saturation process;
- Determine the pipe and heater sizing with power requirements;
- Design of the ice water containing box;
- Choosing sand based on the grain size and its effect on hydraulic and thermal conductivities; and
- The temperature control panel modifications.

Based on several numerical predictions and facilities available, the experimental setup has been fabricated and established, as discussed in the following sections.

### **3.1.1 Pipe Model**

A cylindrical cartridge heater has been utilized as the pipe model in these experiments to model the warm buried pipeline. The cartridge heater has been used instead of a real small diameter

pipe to minimize the electrical noise and the power requirements as shown in Figure 3-2. The heater or pipe model has been buried in the sand medium at various burial depths during the tests.



**Figure 3-2: Cylindrical Cartridge Heater used in the experiment.**

The cartridge heater has the following specifications which has been illustrated in Table 3-1:

**Table 3-1: Cartridge Heater Specifications**

|                  |                    |
|------------------|--------------------|
| Diameter         | 12.6 mm (0.5 inch) |
| Wattage          | 275 Watt (maximum) |
| Brand            | Watlow             |
| Lead End No Heat | 1.97 inches        |
| Accuracy         | +5%, -10%          |
| Volts            | 120                |

### 3.1.2 Soil Box and Soil Type

One of the most important aspects of the experiment setup was to design the test box which has significant effects on the costs, efforts, and time. As estimated in our early numerical simulations, if the soil box dimensions are at least 15 times the pipe diameter, in each direction away from the circumference of the pipe, then the boundary effects become negligible. Table 3-2. summarizes the results of the numerical modeling of the boundary effects by varying the soil box domain size and shows the differences of power obtained between numerical simulations and theoretical shape factor model. If possible, a wider soil box is recommended (20d or 25d) to eliminate the boundary effects even further. While conducting the tests, the soil box contained the soil with the properly positioned heater and thermistors. There is a lid to cover the soil box with the help of a gasket, nuts and bolts. The soil box has been completely sealed and several benchmark tests with dry sand have been carried out using the box. The soil box has been designed to hold vacuum pressures so it can be used to saturate the soil under vacuum as required for the future tests. Figure 3-3 shows a drawing of the soil box and Figure 3-4 shows the soil box filled with dry silica sand (test sand) and buried pipe in it. The soil box used for the test has of following specifications:

- Material: Mild Steel
- Soil Box Dimension:  $1.2\text{m} \times 0.62\text{m} \times 0.36\text{m}$
- Soil used: Silica Sand
- Average Thermal Conductivity of the Soil:  $0.236 \text{ W/m-k}$ .
- Bulk Density of Soil:  $1565 \text{ Kg/m}^3$

**Table 3-2: Thermal boundary effects at different soil box dimensions compared to the shape factor model.**

| <b>Case</b> | <b><math>Q_{\text{pipe}}</math> (W)</b> | <b>Difference from theoretical shape factor model (%)</b> |
|-------------|-----------------------------------------|-----------------------------------------------------------|
| 10d         | 87.08                                   | 2.2                                                       |
| 15d         | 87.98                                   | 1.1                                                       |
| 20d         | 88.2                                    | 0.9                                                       |
| 25d         | 88.36                                   | 0.7                                                       |
| 30d         | 88.66                                   | 0.4                                                       |

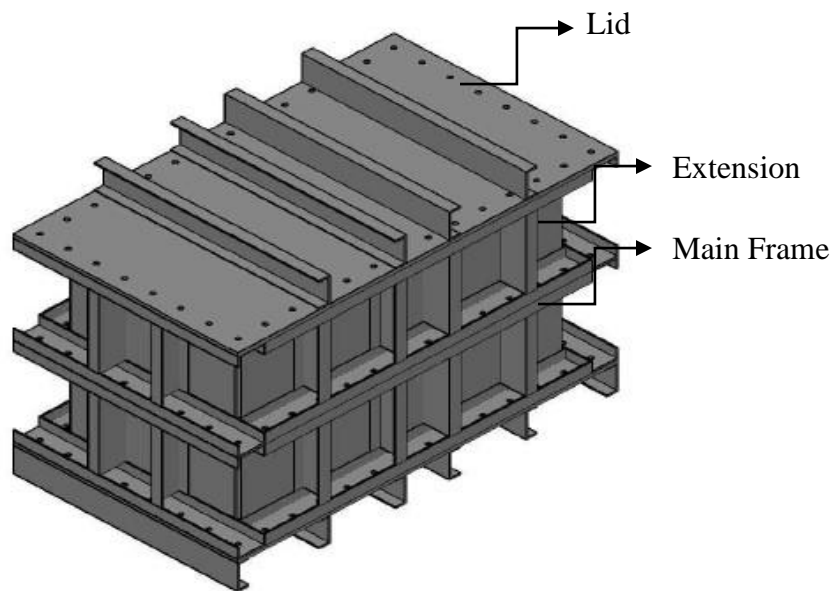


**Figure 3-3: CAD drawing of the soil box.**



**Figure 3-4: Soil box filled with dry sand.**

### **3.1.3 Ice Water Containing Box**

The experimental setup required the boundary temperature to be close to 1°C, to match the ambient temperature presumed in seabed environment. The easiest way to achieve this thermal boundary condition was to insert the test box inside a larger box and fill the space between the walls and bottoms with ice-water mixture. The required size of the outer box was estimated using the amount of energy that needs to be removed from the soil system to achieve the steady state temperature conditions. This depends on the initial temperature of the soil, soil mass, and soil heat capacity; assuming that, the time required for the cooling process is not extremely long and we have access to the required amount of ice. The energy that has to be removed from the soil is:

$$Q_E = mc\Delta T \quad (3.1)$$

And the amount of ice required is:

$$m_{\text{ice}} = \frac{Q_E}{h} \quad (3.2)$$

Where,  $h$  is the ice latent heat.

Figure 3-5 shows the ice-water box which is made of wood. To contain the ice-water mixture and to prevent heat circulation, there is 4 inches of Polystyrene insulation around the box sides, top, and bottom. Also, a continuous polyethylene tarpaulin is used over the insulation to prevent water leakage. After putting crushed ice into the box to a certain level, the soil box has been placed to appropriate position inside it with the help of a 3-ton capacity overhead crane. Then, more ice and water is added into the surrounding gaps. The ice-water mixture has been added in such a way that it maintains 0°C temperature around the soil box. If the temperature starts to go higher than 1°C, more ice blocks in smaller pieces are added to the system to maintain the desire temperature. The box is covered by a lid made with 2-inch-thick polystyrene insulation foam.

The specifications for the wooden box are given as follow:

- Material: Plywood and 2"x 4" lumber
- Dimension: 1.85m × 1.32m × 1.22 m
- Inside Insulation Material: Polystyrene (4-inch thickness)
- Lid: 2-inch Polystyrene Foam.

The ice blocks are made using ice making pans in the cold room facility of the laboratory at a temperature from -20°C to -25°C. The ice pans have the following specifications:

- Materials: Mild Steel (painted)
- Dimension: 0.91 m × 0.91m × 0.13 m



**Figure 3-5: Ice-Water containing box.**

### **3.1.4 Resistance Temperature Detectors (RTD's)**

Resistance Temperature Detectors or RTDs work on the principle that electrical resistance varies with temperature change of RTD elements. They are also commonly referred to as Resistance Thermometer. RTD's are the most accurate sensors for industrial applications and slowly replacing the use of thermocouples in low temperature applications due to their high accuracy and repeatability. Common RTD sensing elements are Platinum, Nickel or Copper and they have repeatable resistances over an operating temperature range (Rosenberg,1994 and Chandra,2015). In this experiment, several RTDs have been used to measure temperatures at different locations of the soil box, pipe model, and boundaries. RTDs are used in this experiment rather than thermocouples because of their wider range of application, higher accuracy, long term stability and good interchangeability. The RTDs are connected to the data acquisition system using male port connector as required by the system. One sample RTD used in the experiments is shown in the Figure 3-6. The operating temperatures of the RTDs ranged from  $-30^{\circ}\text{C}$  to  $100^{\circ}\text{C}$ . The RTDs

also had an accuracy of  $\pm 1$  °C. To ensure the accuracy of the temperature measurement, each RTD was calibrated at different temperature ranging from -5°C to 80°C.

- Number of RTDs used for benchmark test: 14
- Number of RTDs used for Saturated Soil test :18



**Figure 3-6: Resistance Temperature Detector.**

### **3.1.5 Thermal Property Analyzer**

The KD2 Pro-Thermal Property Analyzer has been used to measure the thermal conductivity, thermal diffusivity and volumetric heat capacity of the soil at different conditions. The TR-1 sensor is used to measure the conductivity of the soil as it is generally designed to measure the thermal conductivity of the granular materials. Its large diameter needle helps to minimize the error from contact resistance in granular sample conforming the IEEE 442-03 guide for Thermal Resistivity Measurement. This type of needle usually consists of a heater and temperature sensor.

During measurement, a current is passed through the heater and sensor records the temperatures which are used to measure the thermal conductivity (KD2 Pro Operator's Manual).

To measure the volumetric heat capacity and thermal diffusivity, the dual needle SH-1 sensor is used as shown in the Figure 3-7. Heat is applied to one of the needles for a definite heating time and the temperature is measured in the other needle, the monitoring needle, at a 6-mm distance during the heating and cooling periods.



**Figure 3-7: KD2 Pro Thermal Property Analyzer.**

The specifications are given as follows (KD2 Pro Operator's Manual):

- Operating Temperature:
  - ❖ Controller: 0°C to 50°C

- ❖ Sensors: -50°C to 150°C
- TR1 Sensor (for measuring Thermal Conductivity):
  - ❖ Range: 0.1 to 4.00 W/m-K
  - ❖ Accuracy:  $\pm 10\%$  from 0.2-4 W/m-K,  $\pm 0.02$  from 0.1-0.2 W/m-K
- SH1 –Dual Needle Sensor (for measuring Thermal Diffusivity and Heat Capacity):
  - ❖ Range: 0.1 to 1 mm<sup>2</sup>/s (Thermal Diffusivity) ,0.5-4 MJ/m<sup>3</sup>K (Volumetric Heat Capacity)

Accuracy:  $\pm 10\%$  for both thermal diffusivity and volumetric heat capacity at conductivities above 0.1 W/m-K.

### **3.1.6 Temperature Control Panel and Data Acquisition System**

A temperature control panel with relay control has been installed to adjust the temperature of the pipe model (i.e. the cartridge heater). In the panel, the temperature of the pipe model can be increased or decreased by adjusting the heater current that flows through it. The temperatures from different locations monitored by RTD's have been recorded for post processing using a Data Acquisition System (DAQ) and a computer as shown in. The DAQ system used for the experiments is of following specifications:

- Data Acquisition System
  - ❖ Brand: HBM
  - ❖ Type: QuantumX MX840A universal amplifier boxes
  - ❖ Number of channels available: 24
  - ❖ Sample Rate: For RTDs 1 Hz, For Current 200 Hz
  - ❖ Software Used: Catman

## 3.2 Benchmark Tests

The purpose of the benchmark tests (dry sand tests) was to validate the experimental model using the model developed by Hahne and Grigull (1975) and Thiyagarajan and Yovanovich (1974) which represent Equation (2.6) and Equation (2.7), respectively, and with numerical simulations. Figure 3-1 shows the schematic diagram of the benchmark tests performed to ensure the validity of the model prepared. After placing the sand in thin lifts inside the soil box, 3.2 kPa of pressure was applied manually using a dead weight for every 2 cm of soil bed thickness to ensure uniform density distribution of the sand. Several thermistors were positioned in different locations to capture the temperatures in the different regions of the soil model. The lid of the soil box was completely sealed using gasket and nut-bolts to ensure the dryness of soil medium as it was placed inside the ice-water containing box (Figure 3-5) to maintain the targeted boundary conditions. Before placing the soil box inside the ice water containing box it was ensured to have enough ice below the soil box. After putting ice-water in the surrounding gaps in a fashion to have boundary temperature close to 0°C, the test was started. For each burial depth, at first the heater temperature was set at 25°C and the temperatures from various positions of soil model were recorded. The power of heater was calculated using current amount required to maintain the set temperature of the heater. The heater temperature was gradually increased when the system reached to steady-state for previous temperature setting of the heater. The tests were also conducted backward i.e. decreasing the temperature of the heater gradually (was set to same temperature while increasing) and all steady-state data were recorded for calculations. Several cool down or shut down tests were also performed to analyze the transient response of the pipeline during

shut down. The shut down tests were conducted by turning off the heater from power source and recording all the temperatures while the system was cooling down.

### 3.3 Saturated Tests

The benchmark tests showed deeper burial depths result in better agreement with analytical models. This will be discussed in chapter 4 in more details. So, the saturated tests were performed burying the pipe model (heater) at the depths of 4.04d and 4.48d. Like benchmark test, saturated tests were conducted in both forward and backward directions as well as some cooldown analysis.

#### 3.3.1 Sample Saturation of Test Sand

The experiment was carried out using a container filled with fine silica sands. The weight of dry sand was measured from weight difference of container filled with sand and empty container using platform scale. The thermal conductivity of dry sand was also measured. Then water was allowed to pass from a water container slowly into the sand under atmospheric pressure and controlled by a valve as shown in Figure 3-8. The excess water from the top of container was taken out carefully using paper towel. The water content was also approximated from the mass difference. The parameters for calculations were taken carefully as shown in Table 3-3.

**Table 3-3:Parameters obtained from sample saturated test.**

|                             |       |
|-----------------------------|-------|
| Void Ratio, $e$             | 0.7   |
| Relative Density, $D_r$     | 82.8% |
| Porosity of Sand, $n$       | 0.41  |
| Degree of Saturation, $S_r$ | 66.5% |

The degree of saturation obtained from the test was 66.5 %, and as discussed before, several previous studies reported that under atmospheric pressure the degree of saturation may be increased by displacing air in sand with CO<sub>2</sub>, slow permeation from the base up, de-airing water before introducing into sand, and passing several pore volumes of water through the sample. Several studies discussed thermal conductivity and hydraulic conductivity increases sharply up to approximately 70% of the degree of saturation of the soil (Zhang, 2014 and Tarnawski et al, 2013). Because of having 66.5% degree of saturation of the sand used from the sample test, the future tests were conducted using sand saturated under atmospheric pressure rather than using vacuum.



**Figure 3-8: Sample test to measure degree of saturation of test.**

### 3.3.2 Saturated Tests

Table 3-4. shows the parameters and test conditions of the conducted saturated tests.

**Table 3-4:Parameters obtained from sample saturated test.**

| Test             | Test Condition                                                                                                                                                        |
|------------------|-----------------------------------------------------------------------------------------------------------------------------------------------------------------------|
| Uniform test     | Uniform saturated sand at burial depth, D/d= 4.04. Grain size: maximum 0.7 mm, minimum 0.08 mm.                                                                       |
| Open trench test | The heater placed in the open trench at same depth i.e. D/d= 4.04, no backfill.                                                                                       |
| Backfill test 1  | The trench is backfilled with larger grain size sand than the native sand at burial depth, D/d= 4.04. Grain size: maximum 0.84 mm, minimum 0.5 mm.                    |
| Backfill test 2  | The condition is same as Backfill test 1 except at a greater burial depth of D/d= 4.46. Grain sizes: maximum 0.84 mm, minimum 0.5 mm.                                 |
| Backfill test 3  | The trench is backfilled with larger grain size sand than Backfill test 1 and Backfill test 2 at burial depth, D/d= 4.04. Grain Sizes: maximum 2.0 mm, minimum 1.4 mm |

Table 3.5. shows the hydraulic conductivity coefficient obtained using D10 and D60 value of the sands after sieve analysis. D10 and D60 values are widely used for gradation of the soil. D10 is the grain diameter at 10% passing and D60 is the grain diameter at 60% passing. D10 is also called effective grain size, which gives a good indication of the permeability characteristics of a coarse-grained soil and can be obtained as (Craig,2013):

$$K = D_{10}^2 * 10^{-2} \tag{3.3}$$

Table 3-5. illustrates the hydraulic conductivity coefficients for different sands use in the experiments. Hydraulic conductivities can be obtained using Eq. (3.3) using the D10 value obtained through sieve analysis of the sands.

**Table 3-5:Hydraulic Conductivity Coefficient Table.**

| <b>Sand Type</b>          | <b>Grain Sizes(mm)</b> | <b>D10, D60(mm)</b> | <b>Hydraulic Conductivity Coefficient (m/s)</b> |
|---------------------------|------------------------|---------------------|-------------------------------------------------|
| Native                    | 0.08-0.7               | 0.12,0.21           | $1.44 \cdot 10^{-4}$                            |
| Backfill 1 and Backfill 2 | 0.5-0.84               | 0.42,0.61           | $1.764 \cdot 10^{-3}$                           |
| Backfill 3                | 1.4-2                  | 1.5,1.8             | $2.25 \cdot 10^{-2}$                            |

### 3.3.2.1 Uniform Test

Test sand was added in the same fashion as benchmark tests after placing coarser sand of 1.1 cm thickness in between two Geotextile layers at the bottom of soil box as shown in Figure 3-9.

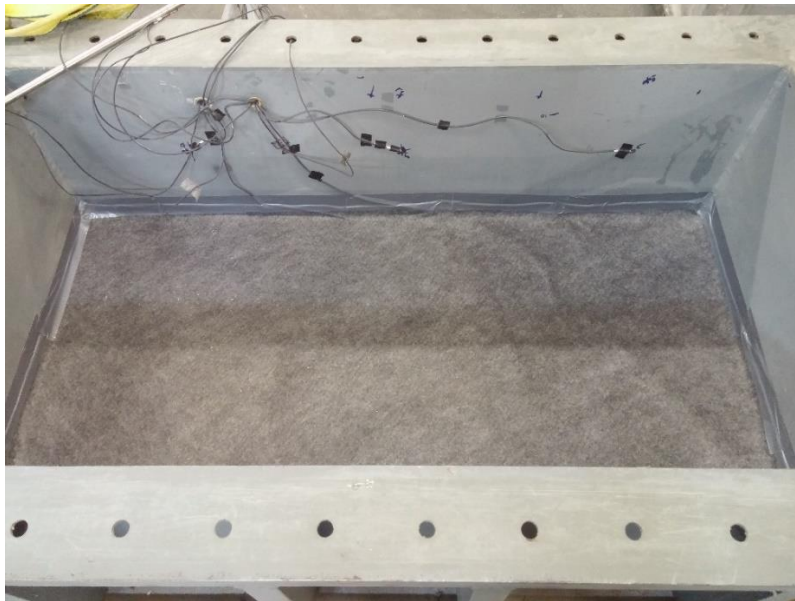


**Figure 3-9: Empty Soil box with RTD's positioned and coarser sand below Geotextile.**

The Geotextile layer with coarser sand at the bottom worked as a filter and also ensured the even allowance of water flow through the soil box. Same amount of pressure was applied using dead weight as benchmark tests. The heater was positioned at designated burial depth and several thermistors were positioned properly. A water tank with tubing and valves was connected to the soil box to pass water slowly from the bottom of the soil box. The clearance between top of the soil box and soil surface was 10 cm as shown in Figure 3-10. Water level indicator installed at the other side of the box showed the water level inside the soil box. The water was allowed to pass very slowly maintaining 15 cm of water head difference to avoid piping and disturbances in sand.



**Figure 3-10: Saturation of test sand.**

After saturation, the following parameters were calculated for dry sand density of  $1448 \text{ Kg/m}^3$  as presented in Table 3-6.

**Table 3-6: Parameters obtained from uniform saturation test.**

|                             |        |
|-----------------------------|--------|
| Sand Type                   | Silica |
| Burial Depth, $D$           | 4.04d  |
| Void Ratio, $e$             | 0.84   |
| Relative Density, $D_r$     | 35.25% |
| Porosity of Sand, $n$       | 0.46   |
| Degree of Saturation, $S_r$ | 60.1%  |

Here, the relative density was calculated using prior test data of maximum void ratio and minimum void ratio for the same test sand. More water was added slowly so that the soil medium became submerged under water which protected the soil medium from exposing to atmospheric

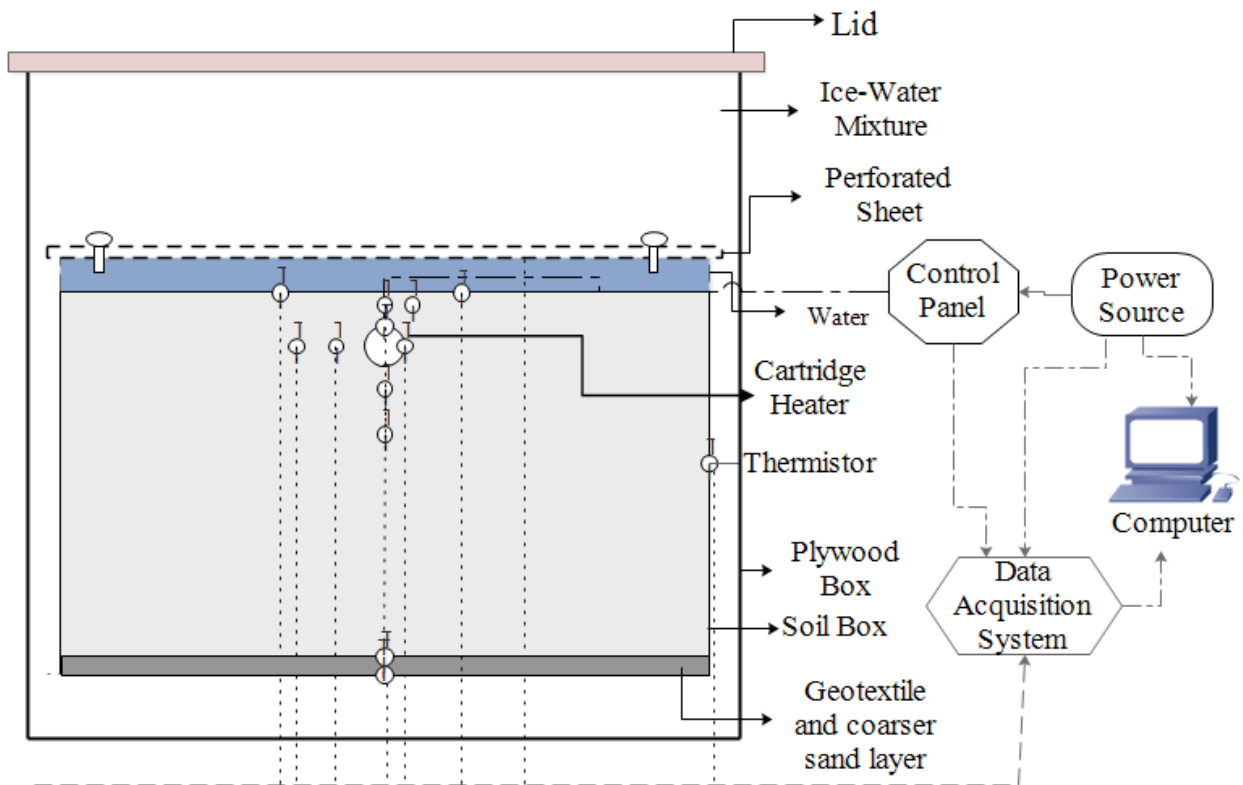


**Figure 3-11: Schematic diagram for uniform saturated sand test.**

air and decreasing degree of saturation of sand. Before placing the soil box inside the ice water containing box, enough ice was placed below the soil box. A perforated sheet as shown in Figure 3-11 protects the soil bed from any disturbances that might occur during adding ice blocks while allowing for natural convection to take place smoothly. After putting ice-water in the surrounding gaps of the ice-water box in a fashion to have boundary temperature close to 0°C, the test was started.

### 3.3.2.2 Open Trench Test

One open trench test i.e. without backfilling the trench was performed at the same burial depth of the uniform soil test to check the behavior of the model. A trench of slope ratio 1:1 was aimed to excavate using a custom-made trench tool fabricated from high-density polyurethane board as



**Figure 3-12: Trenching in sand.**

as shown in Figure 3-12. But the actual slope was obtained 1.7:1 because the soil was left over the shoulders and washed down the slope, making it less steep. At the time of trenching the sand medium was kept under water to maintain the same degree of saturation achieved before. The relative density of the sand was quite low as shown is Table 3-6. and waves were also generated during movement of the soil box. So, all the trenching works were done inside the ice water containing box after placing the soil box at proper position. Enough ice at the bottom of the soil box was ensured before starting the trenching work and the thermistors and heater were also placed carefully. The heater temperature was set to 10°C at first and because of the power requirement of the heater it gradually increased up to 23.71°C. Figure 3-13 shows the heater placed in the open trench without backfill.



**Figure 3-13: Pipe or heater placed in open trench.**

### 3.3.2.3 Backfill Tests

After the open trench test, three backfill tests were carried out at two burial depths of  $D/d= 4.04$  and  $D/d= 4.46$  to investigate the behavior of the model. The backfill sands were saturated following the same procedure described in section 3.3.1 in a small container under atmospheric pressure. The trench was then filled with the saturated backfill sand carefully (Figure 3-14). Several thermistors were positioned at different locations and the data from them recorded accordingly. Same grain size sands were used for Backfill test 1 and 2 and larger grain size sand was used for Backfill test 3 as illustrated at Table 3-4. The slope ratio was 1.7:1 for backfill test 1 and backfill test 2 but 1:1 for backfill test 3. The aim of trenching was to create the slope of ratio 1:1 but during trenching before open trench test the soil was left over the shoulders and made the slope less steep. But during second trenching after backfill test 2, it was ensured to have the slope ratio 1:1 in the trench.



**Figure 3-14: After backfilling the trench.**

# Chapter 4

## 4 Results and Discussions

### 4.1 Benchmark Tests Result and Validation

The experimental model has been validated using the results from benchmark tests and the model developed by Hahne and Grigull (1975) as explained in section 2.2. Figure 4-1 shows the power required by the heater (pipe model) per unit length, varying the temperature difference at different burial depths,  $d$ . The curves imply the deviation from the analytical result is greater at shallower depths of buried pipe, for example  $D/d=0.79$ , and the error decreases as the burial depth increases. This is since for the shallow burial depths the pipe model is close to the lid of the box, so the power requirements may fluctuate significantly because the boundary temperatures were controlled manually using ice blocks. For deeper burial depths, as the soil bed thickness increases, steady state power requirements have been observed. The maximum average percentage of error was observed for burial depth,  $D/d=0.79$  (i.e. around 8.1%) and the minimum average percentage of error was 3.7% for  $D/d=5$ . The shape factors obtained from the experimental results of benchmark tests have been made dimensionless choosing heater or pipe length as the length scale. Dimensionless shape factors decrease with an increase in the burial depth. Figure 4-2 shows the trend of dimensional shape factor for experimental outputs and analytical model results obtained from benchmark tests using different burial depths, where, constant temperature boundary condition is the model proposed by Hahne and Grigull (Equation

2.6) and constant flux boundary condition is the model developed by Thiyagarajan and Yovanovich (Equation 2.7).

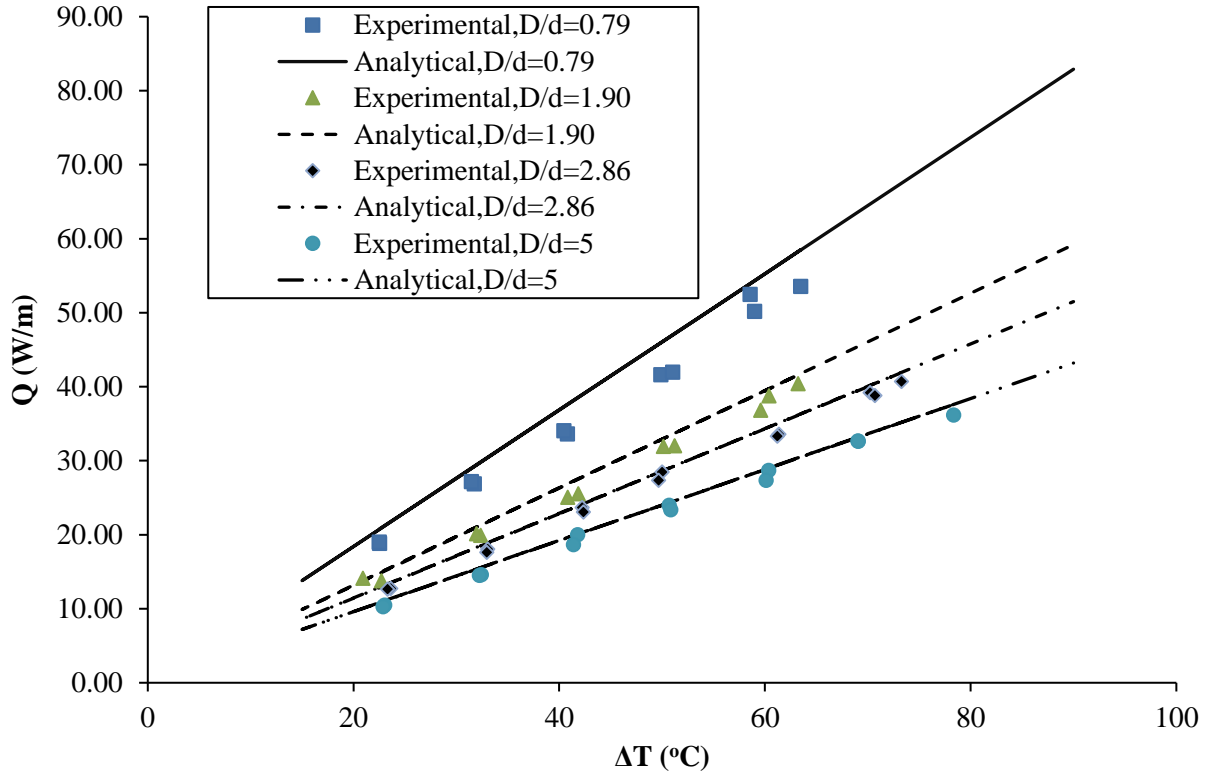


**Figure 4-1: Power vs. boundary temperature difference graph at different burial depths for benchmark tests.**

Shapiro-Wilk's test (Royston,1992) confirms that the outputs for both analytical Hahne and Grigull (1975) model and experimental models are normally distributed. Though the sample size is small as the tests are time consuming, after satisfying the assumptions of Welch's t-test (Johnson and Wichern,1992) it confirms that at 95% confidence interval the null hypothesis (i.e. both means are the same) is true as the p value becomes 0.733.

Using the accuracy of  $\pm 10\%$  for Cartridge Heater and Thermal Property Analyzer as suggested by the manufacturer, the evaluated maximum uncertainty was 14.14% for the experimental set

up. Figure 4-2 also, shows that the analytical results fall between the uncertainty margin which proves the legitimacy of the experiments.

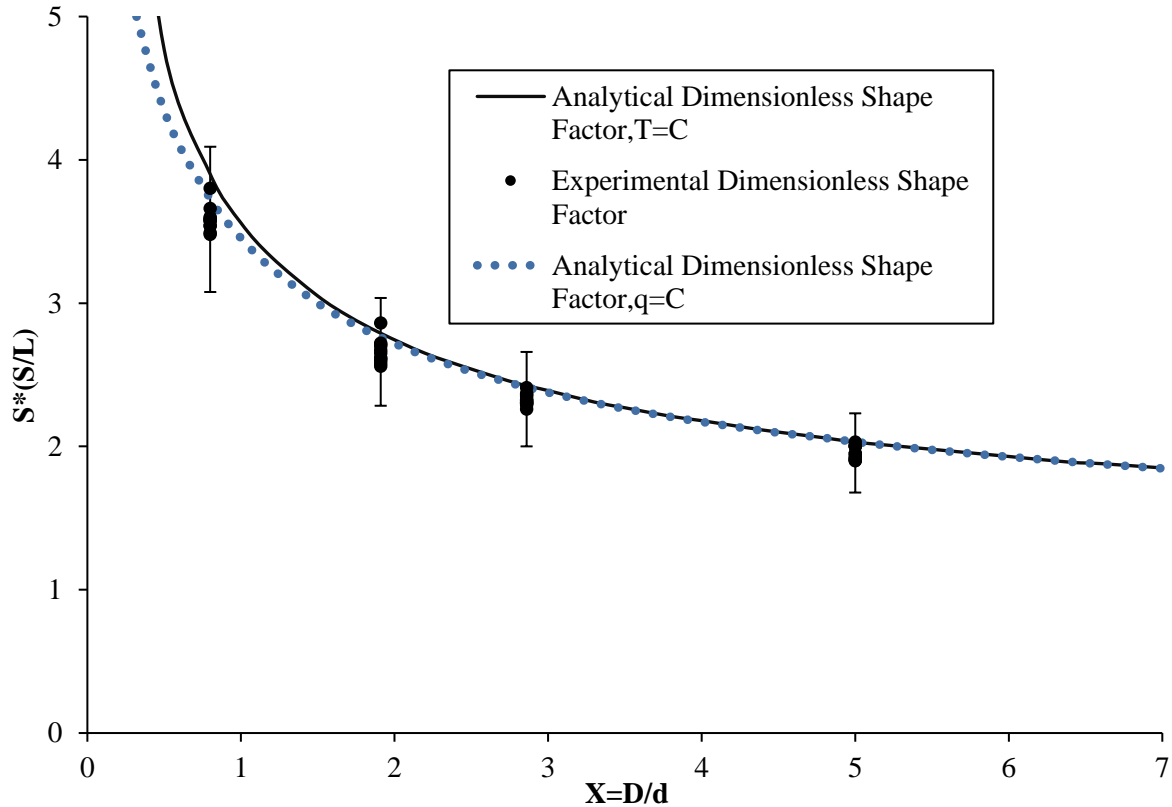


**Figure 4-2: Dimensionless shape factor comparison for different burial depths from benchmark tests.**

A family of cool down curves of pipe wall temperatures is shown in Figure 4-3 for a burial depth of 5d. The figure illustrates the behavior of buried pipes after shutdown for benchmark tests (dry sand tests) using three different pipeline initial temperatures. The general thermal response follows the typical cool down trend shown in Figure 1-2. The temperature of the pipeline should not fall below the critical temperature as that will lead to flow assurance issues such as hydrate formation. The shut down tests have been performed by disconnecting the heater from the power source and recording the temperatures until they have reached a steady state.

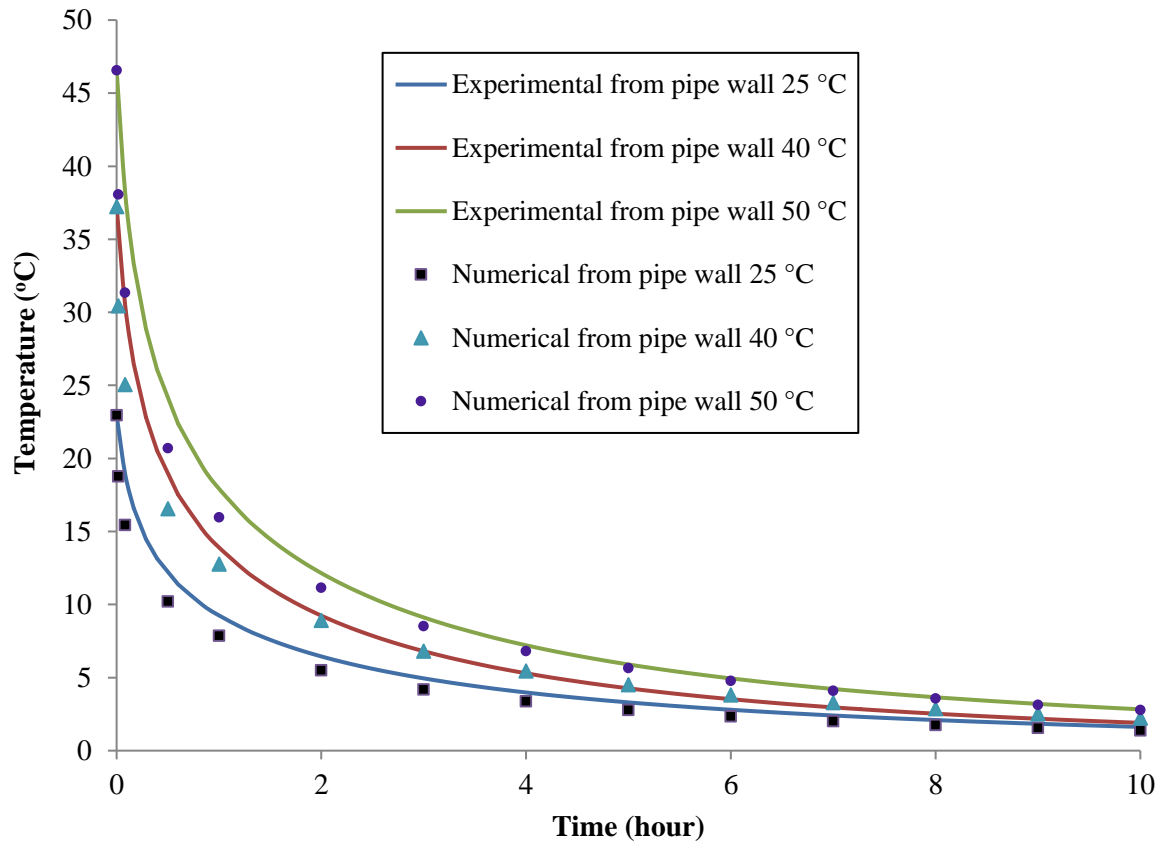


**Figure 4-3: Cool down curves of pipe wall for burial depth of 5d from benchmark tests.**

A series of CFD simulations have also been carried out for the same thermal conditions. The CFD simulations fall outside of the scope of the present thesis and are discussed in detail in another publication (Haghighi et al, 2017). The results of the numerical modeling are also in good agreement with the experimental results as shown in Figure 4-3. The numerical model assumes the heat dissipation is through the surrounding medium of the buried pipe and ignores the thermal energy stored in the pipeline. This leads to a small difference from the experimental results, but the overall difference is under 10%.

## 4.2 Saturated Tests Result

Figure 4-4 and Figure 4-5 represent the power required by the heater (pipe model) per unit length based on a set pipe wall temperature. For the saturated tests, the curves (Figure 4-4 to Figure 4-6) are drawn for power per unit length of the heater versus average pipe wall temperature. As the top boundary (i.e. top water surface) is 10 cm away from the soil bed and close to zero degree ( $0^{\circ}\text{C}$ ) Celsius temperature, average pipe wall temperature has been used in the horizontal axis of those curves. Four tests were performed with the same burial depths (i.e. uniform test, open trench test, backfill test 1 and backfill test 3). One backfill test (i.e. backfill test 2) was carried

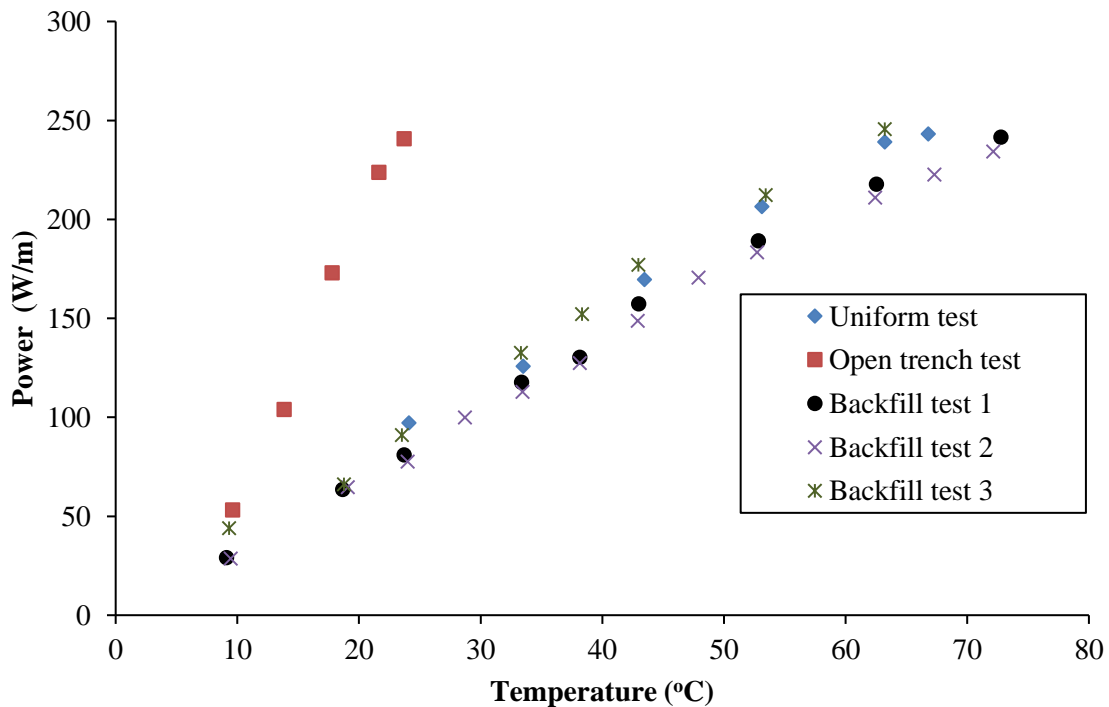


Figure 4-4: Power vs. pipe wall temperature curves for forward tests.

out at higher burial depth (i.e.  $D/d= 4.46$ ). Power requirement for the open trench test should be high as the pipe was exposed to water and significant heat loss can be monitored due to convection. But it can be seen from Figure 4-4 and Figure 4-5 that the power requirement for the uniform test was high compared to the backfill test 1 and backfill fill test 2. As larger grain size sand was used to backfill the trench than the native sand, more water became trapped in that area which reduces the overall thermal conductivity in that region. However, the porosity of the backfill sand was not high enough that would allow the trapped water to circulate and generate significant natural convection. Backfill test 3 shows the effect of natural convection in the system as larger grain size sand used for backfilling the trench in this case. The porosity and permeability of the backfill sand were large enough which allowed the trapped water to circulate and induce natural convection. Further increase in grain size of the backfill sand will further increase heat loss due to significant natural convection as observed by far in the tests.

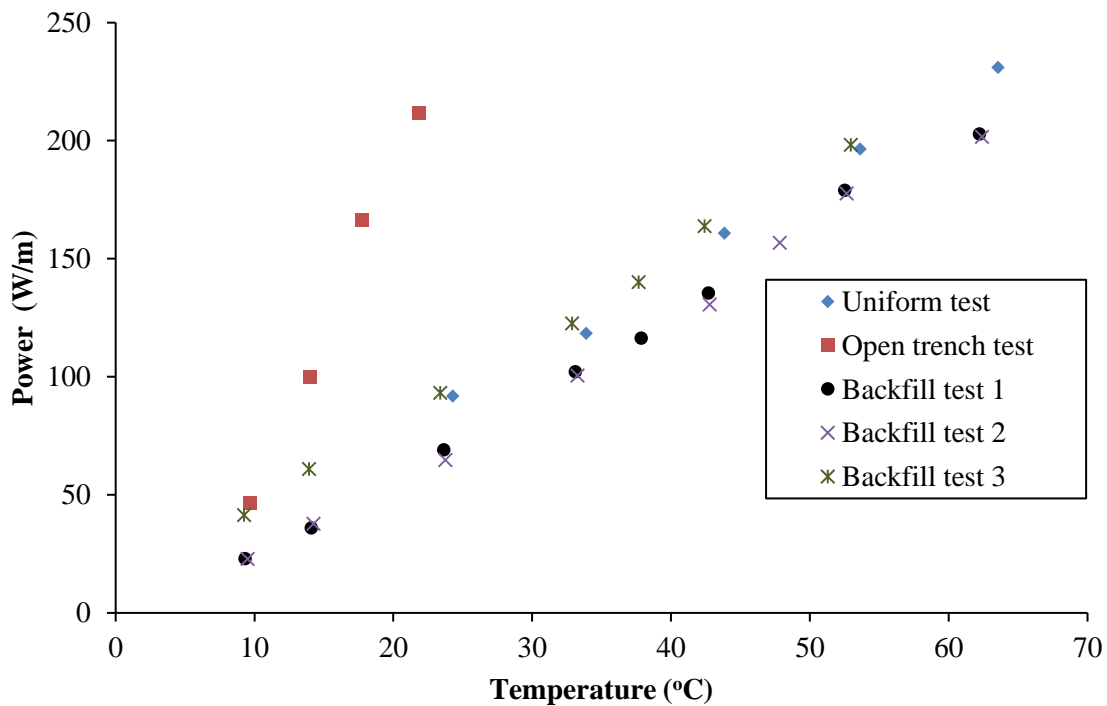
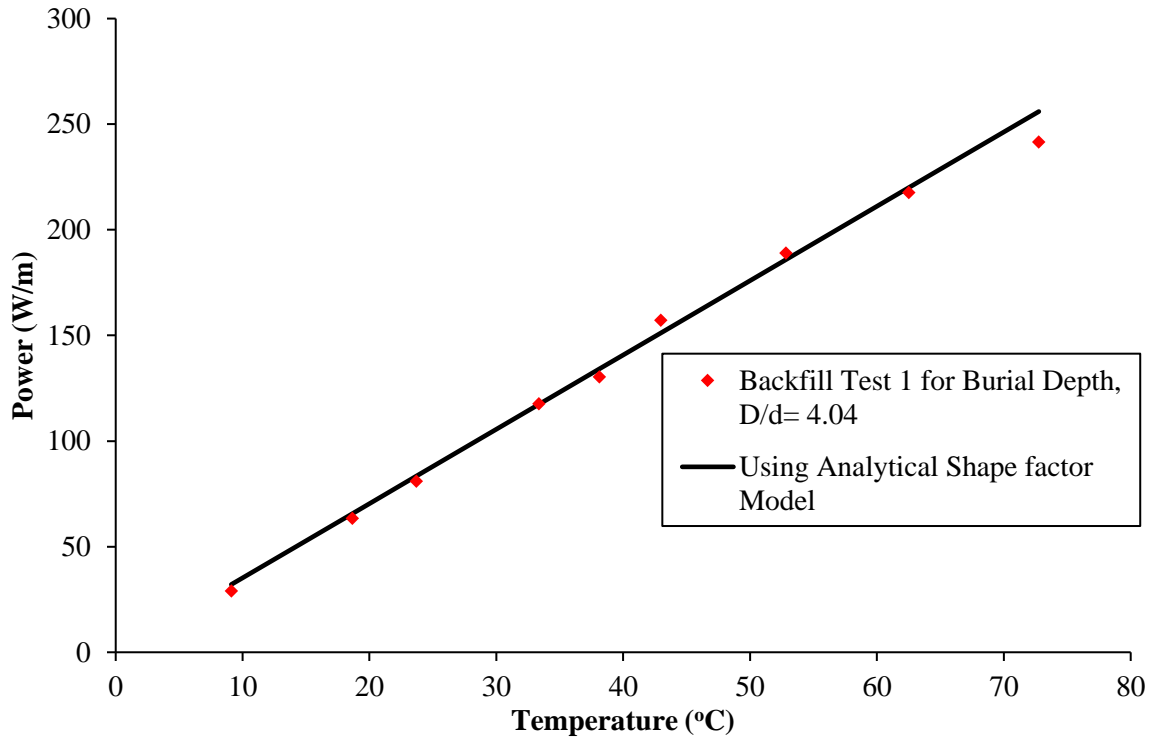


Figure 4-5: Power vs. pipe wall temperature curves for backward tests.

The overall thermal conductivity measured in the backfill zone for backfill test 1 and backfill test 2 were lower than the native sand which also implies less heat dissipation through the backfill area. In case of backfill test 2, as the burial depth for backfill test 2 is higher than the backfill test 1, lower heat loss can be seen in Figure 4-4 and Figure 4-5 for backfill test 2. Because of the greater burial depth, soil bed thickness is greater in case of backfill test 2 which provides more thermal insulation.

For backfill test 3, larger grain size sand was used than the backfill test 1 and backfill test 2. The hydraulic conductivity coefficient of the backfill sand used in this test is much higher than the backfill sand used for backfill test 1 and backfill test 2. Figure 4-4 and Figure 4-5 illustrate that power requirement per unit length of heater is higher for backfill test 3 than the uniform test. The effect of natural convection can be seen from backfill test 3. The permeability and porosity of the backfill sand used for this test allows the trapped water to circulate and induce heat loss through natural convection. However, the heat loss through natural convection was less in this case but use of larger grain size sand for backfilling can lead to significant heat loss.

Figure 4-6 represents a comparison of the power requirement per unit length at different pipe wall temperatures between experimental outputs and using the shape factor model. The results obtained from the shape factor model (Hahne and Grigull,1975) are very close to the results obtained from the backfill test 1 for burial depth,  $D/d= 4.04$ . The permeability and porosity of backfill soil used in this case were not high enough compare to the native sand to allow the natural convection. As the shape factor model is based on the heat loss through conduction, so it can be concluded that, in the backfill test 1 and backfill test 2, the overall heat loss reduced compared to the uniform test and conduction was more dominant over natural convection.



**Figure 4-6: Power comparison between backfill test 1 (saturated) and analytical shape factor model for  $D/d=4.04$ .**

### 4.3 Saturated Tests Cooldown Curves

The heat loss mechanisms through the process discussed above are from steady state analysis. Transient response of the pipeline is also important to capture shutdown phenomena and ensuring the production flow temperature does not fall below the critical temperature, as that will lead to flow assurance issues such as hydrate formation (Sadegh et al, 1987).

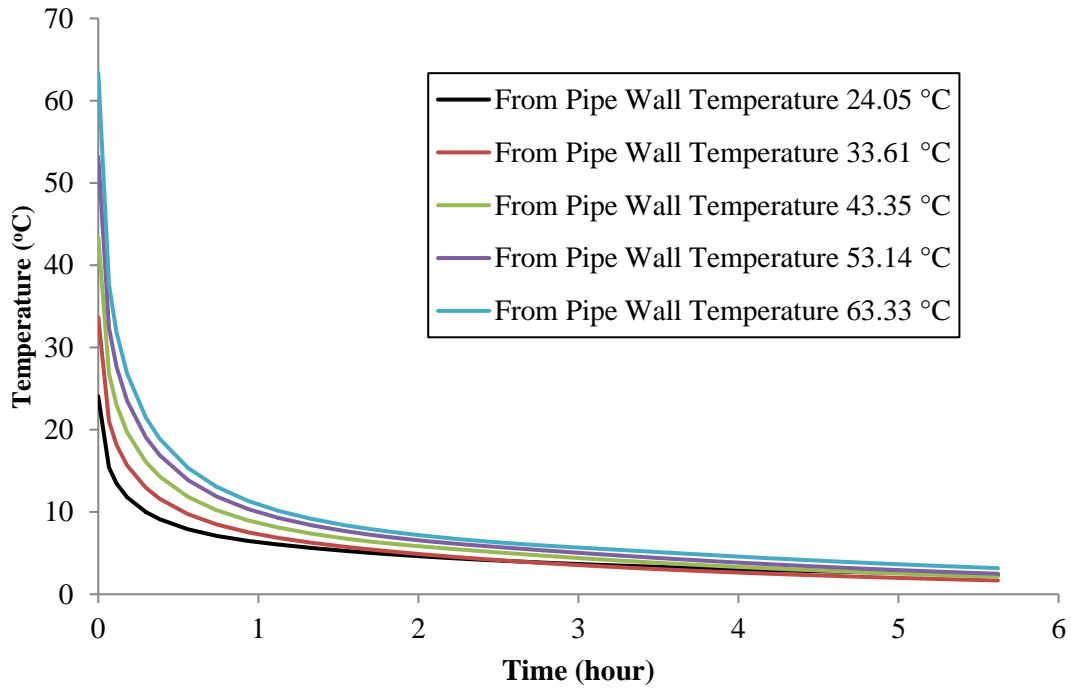


Figure 4-7: Cool down curves of pipe wall for uniform test.

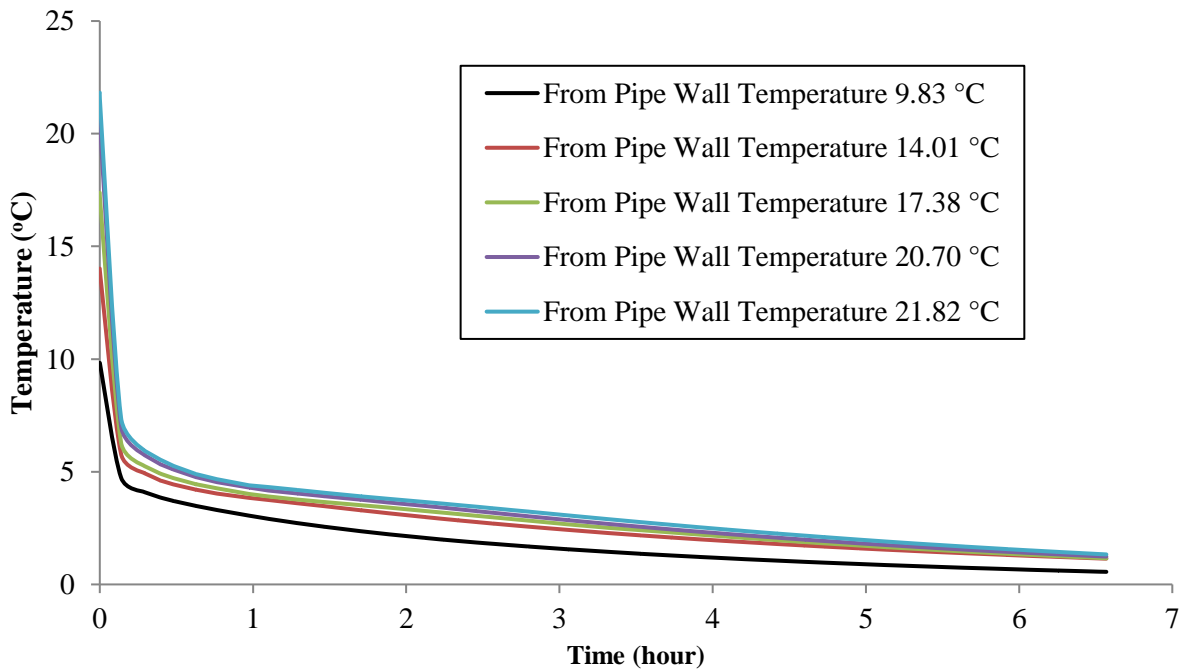


Figure 4-8: Cool down curves of pipe wall for open trench test.

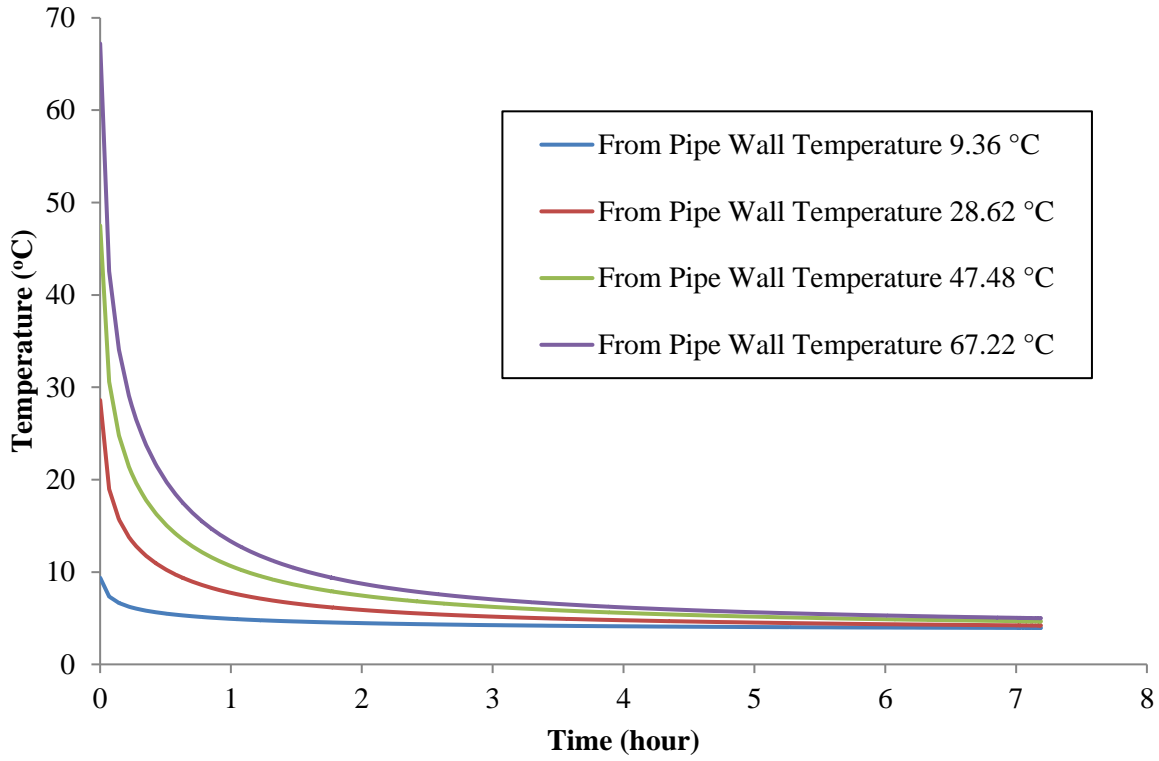


Figure 4-9: Cooldown curves of pipe wall for backfill test 1 at burial depth,  $D/d=4.04$ .

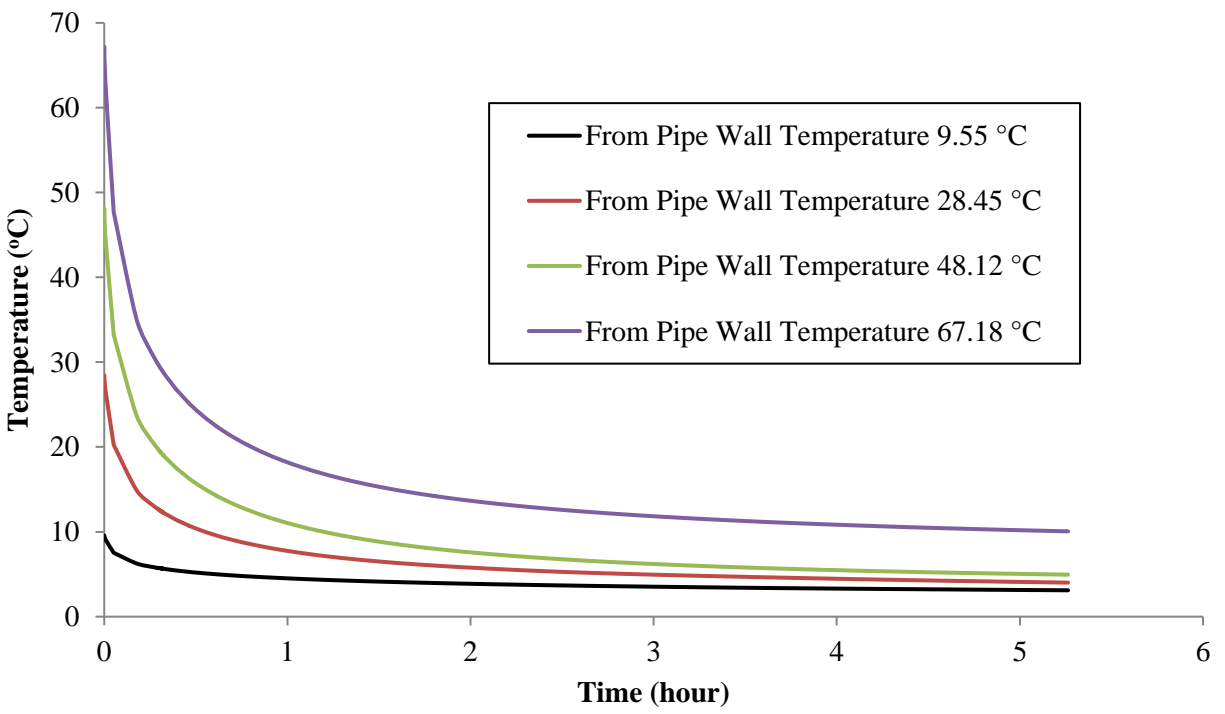
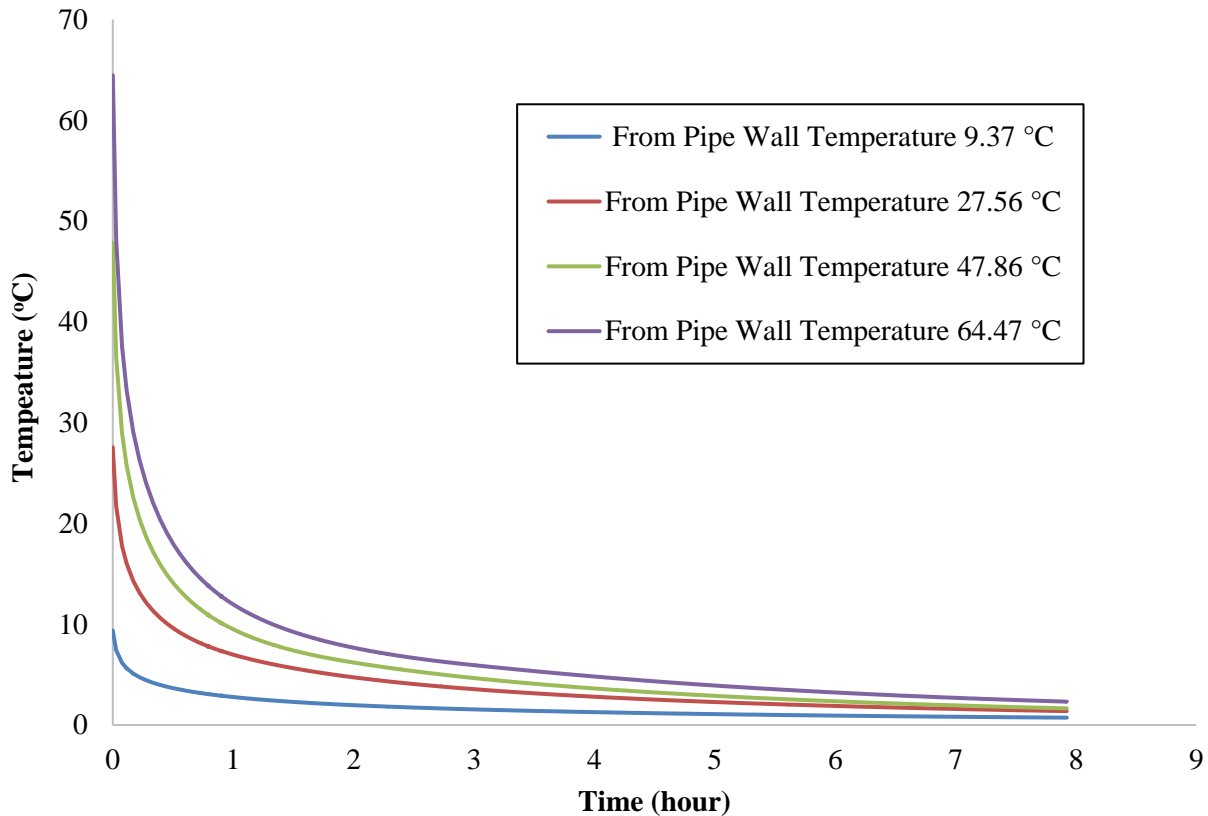
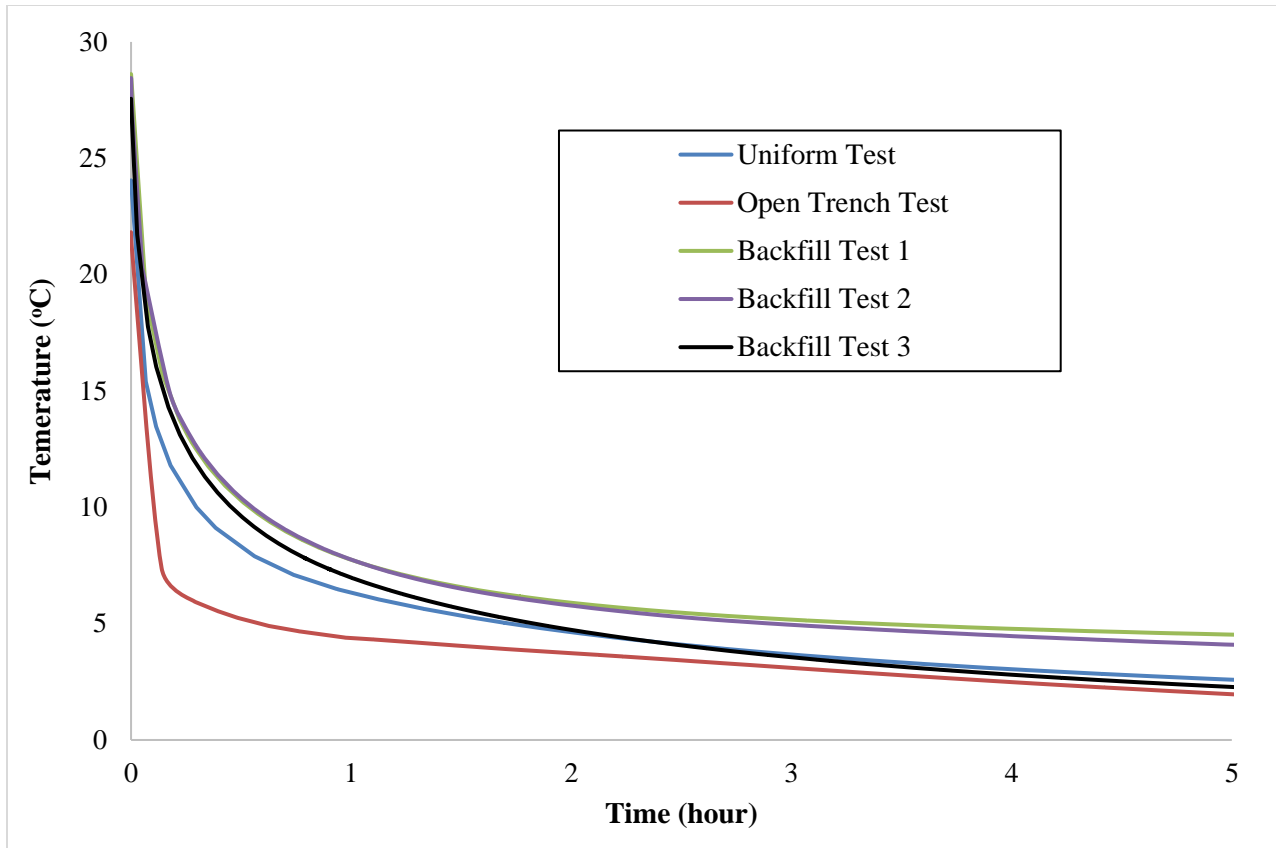


Figure 4-10: Cooldown curves of pipe wall for backfill test 2 at burial depth,  $D/d=4.46$ .



**Figure 4-11: Cooldown curves of pipe wall for backfill test 3 at burial depth,  $D/d=4.04$ .**

Shutdown tests were performed for each saturated sand tests to capture the transient behaviour of the model. More detailed CFD simulations will be performed in future studies to understand the effects of various backfill conditions on the production cooldown process. Figure 4-7 and Figure 4-8 show the temperature response with respect to time during shutdown for uniform test and open trench test. During open trench test the pipeline was fully exposed to water and sudden temperature drop can be observed from Figure 4-8 due to high convective heat transfer coefficient of water. Figure 4-9 to Figure 4-11 show the thermal response of backfill tests performed for three conditions during cool down tests. The general thermal response follows the typical cool down trend shown in Figure 1-2.



**Figure 4-12: Cooldown curves for different saturated tests.**

Figure 4-12 shows the cooldown curves generated from different saturated tests. It is visible from the figure that for backfill test 1 and backfill test 2 the no touch time is more which was discussed in the section 1.1 of this thesis. But for backfill test 3 as natural convection is taking place the temperature is decreasing faster than backfill test 1 and backfill test 2. This may lead to fall the pipeline temperature below critical temperature and inducing several flow assurance issues. The cool down time is important and should be large enough to provide the pipeline operators sufficient time to find and fix issues. The shut down tests have been performed by disconnecting the heater from the power source and recording the temperatures until they have reached a steady state.

# Chapter 5

## 5 Conclusions

This chapter presents a review of the main contributions of this thesis in flow assurance modelling for offshore oil and gas applications. Recommendations for future work with practical implementation is briefly proposed in this chapter as well.

### 5.1 Review of Important Observations

The present thesis is mainly focused on the experimental modelling of the heat loss mechanism from offshore buried pipelines in a semi-infinite porous medium. The main contributions of the thesis can be described as follows:

- The thesis includes a literature review relevant to the heat loss mechanism from offshore buried pipeline and describes different theoretical models proposed by various researchers, as well as the current gaps in knowledge e.g. lack of heat transfer models for buried pipelines in saturated soil medium.
- Previous works related to heat loss from offshore buried pipeline were solely focused to conduction problem only. This research aimed to draw attention regarding effect of natural convection in the heat loss mechanism from offshore buried pipeline.
- Design of experiments and experimental setup were challenging tasks and detail description of the process involved with those are discussed in detail in the thesis.

- Validation of the experimental model was performed utilizing analytical shape factor models and early performed numerical analysis. Two steps validation of the model proves the legitimacy of the experimental analysis.
- Statistical and Uncertainty analysis were also performed to ensure the normal distribution of the experimental outputs. The experimental results obtained from the benchmark tests fall between the uncertainty margin which also establish the statistical stability of the outputs.
- Benchmark tests showed deeper burial depths result in better agreement with analytical models. We choose burial depth in a range of 3d to 5d for our further saturated experiments.
- A Sample test was carried out to check the degree of saturation of the native sand obtained through the saturation process under atmospheric pressure. The degree of saturation of sand obtained through sample test was 66.5%. The sands for future saturated tests were saturated under atmospheric pressure as prior studies reported that, thermal conductivity and hydraulic conductivity increases sharply up to 70% (approximately) of the degree of saturation of the sand.
- Five different saturated tests were performed at two different burial depths. Heat loss through natural convection can be significant if the porosity and permeability of the backfill sand are large enough to allow circulation of the trapped water. The thesis also shows that overall heat loss can be less than the uniform test (without backfill) if the trapped water in the backfill sand can not circulate as the overall heat transfer coefficient decreases in this case. However, with further increase in the grain size it is expected that greater heat loss will happen due to increase in the natural convection.

## 5.2 Future Recommendations

In conclusion, the results from this testing program look promising and are currently being used to plan and design the upcoming tests. Several recommendations can be proposed to carry out future tests and establishing very useful model to calculate heat loss from offshore buried pipeline.

- All the tests were conducted using only one heater or pipe model of same power. Multiple heaters of different powers and same power can be used to investigate the heat loss on superimposed temperature fields.
- Two trench angles of slope ratio 1.7:1 and 1:1 were used to trench and burying the pipe. Experiments with several trench angles will make model more suitable and will provide valuable prediction of heat loss from offshore buried pipelines.
- As the soil type can vary from clay to gravel in offshore conditions, more tests using a wide range of backfill soil will increase the applicability of the experimental model.
- Degree of saturation of the native and backfill soil can be increased by saturating them under vacuum. Future tests with higher degree of saturation of soil will catch more actual heat loss mechanism in offshore condition.
- As the experiments demand additional time, numerical modelling can be a good choice in this regard which can save in cost and time. The results from experimental outputs can be compared with numerical model and the validated numerical model can be utilized widely through industry as a tool in pipeline design for offshore buried pipelines.
- Development of new correlations or models for heat loss from offshore buried pipeline can be another important prospect for future research.

# List of Publications from this Thesis

## Conference Papers:

Chakraborty, S., Talimi, V., Muzychka, Y., McAfee, R., and Piercey, G., 2016, Design of Experiment and Validation of Model for Offshore Buried Pipeline Thermal Analysis, *in proceedings of the International Pipeline Conference*, 26-30 September, Calgary, Canada.

Chakraborty, S., Talimi, V., Muzychka, Y., and McAfee, R., 2016-C, Modeling of Heat Loss from Offshore Buried Pipeline through Experimental Investigations and Numerical Analysis, *in proceedings of the Arctic Technology Conference*, 24-26 October, St.John's, Canada.

Chakraborty, S., Talimi, V., Haghghi, M., Muzychka, Y., and McAfee, R., 2016, Thermal Analysis of Offshore Buried Pipelines through Experimental Investigations and Numerical Analysis, *in Proceedings of the ASME 2016 International Mechanical Engineering Congress and Exposition*, November 11-17, Phoenix, Arizona, USA.

## Journal Paper:

Chakraborty, S., Talimi, V., Muzychka, Y., McAfee, R., Haghghi, M. and Piercey, G., "To be submitted", *International Journal of Heat and Mass Transfer*.

# Bibliography

Archer, R.A. and O'Sullivan, M.J., 1997, Models for Heat Transfer from a Buried Pipe, *Society of Petroleum Engineers, Inc.*, **Volume 2**: SPE 36763.

Atwan, E.F., Sakr, R.Y., 2005, Natural Convection Heat Transfer from a Heated Pipe Embedded in a Liquid-Saturated Porous Medium, *Engineering Resource Journal*, **Volume 98**: pp M52-M69.

Barletta, A., Zanchini, E., Lazzari, S., & Terenzi, A. (2008). Numerical study of heat transfer from an offshore buried pipeline under steady-periodic thermal boundary conditions. *Applied thermal engineering*, 28(10), 1168-1176.

Bau, H. H., & Sadhai, S. S., 1982, Heat Losses from a Fluid Flowing in a Buried Pipe, *International Journal of Heat and Mass Transfer*, **Volume 25(11)**: pp 1621-1629

Bejan, A. (2013), *Convection heat transfer*, John wiley & sons.

Cass, A., Campbell, G. S., & Jones, T. L. (1984). Enhancement of thermal water vapor diffusion in soil. *Soil Science Society of America Journal*, **48(1)**, 25-32.

Chandra J., 2015, *Thermal Sensors Principles and Applications for Semiconductor Industries*, Springer, New York.

Craig, R. F. (2013), *Soil mechanics*, Springer.

de Lieto Vollaro, R., Fontana, L., & Vallati, A. (2011). Thermal analysis of underground electrical power cables buried in non-homogeneous soils. *Applied Thermal Engineering*, 31(5), 772-778.

de Lieto Vollaro, R., Fontana, L., Quintino, A., & Vallati, A. (2011). Improving evaluation of the heat losses from arrays of pipes or electric cables buried in homogeneous soil. *Applied Thermal Engineering*, 31(17), 3768-3773.

Dupuit, J. É. J., 1863, *Études théoriques et pratiques sur le mouvement des eaux dans les canaux découverts et à travers les terrains perméables: avec des considérations relatives au régime des grandes eaux, au débouché à leur donner, et à la marche des alluvions dans les rivières à fond mobile*. Dunod.

Ewida, A. A., Hurley, S. J., Edison, S. H. and The, C. E., 2004 ,Shallow to Deepwater Facilities and Flow Assurance Challenges in Offshore Newfoundland, in *Proceedings of the Fourteenth International Offshore and Polar Engineering Conference*, Toulon, France.

Forchheimer, P. ,1901, Wasserbewegung durch boden. *Z. Ver. Deutsch. Ing*, **Volume 45(1782)**: pp 1788

Guo, B., Song S., Chacko, J. and Ghalambor, A., 2005, *Offshore Pipelines*, Elsevier Science, Burlington, pp 175-180.

Haghighi, M., Talimi, V.,Chakraborty,S., 2017, Investigation of Heat loss from Pipes Buried in Seabed, in the proceedings of the 2nd Thermal and Fluid Engineering Conference, TFEC2017, April 2-5, 2017, Las Vegas, NV, USA

Hahne, E., Grigull, U., 1975, Formfaktor und Formweiderstand der stationaren mehrdimensionalen Wärmeleitung, *International Journal of Heat and Mass Transfer*, **Volume 18**: pp 751.

Holman, J. P., 1966, *Experimental Methods for Engineers*, McGraw-Hill USA , Chapter 3, Eighth Edition.

Johnson R.A., & Wichern D. W., 1992, *Applied multivariate statistical analysis*, Englewood Cliffs, NJ: Prentice hall, pp 284-286, Chap. 6.

KD2 Pro Operator's Manual, Version 12, Decagon Devices Inc., USA.

Nield, D. A., and Bejan, A., 1999, *Convection in Porous Media*, 2nd edition, Springer-Verlag, New York.

Randolph, M. F., Gaudin, C., Gourvenec, S. M., White, D. J., Boylan, N., & Cassidy, M. J., 2011, Recent advances in offshore geotechnics for deep water oil and gas developments, *Ocean Engineering*, **Volume 38(7)**: pp 818-834.

Rosenberg R. J. ,1994, Temperature measurement on the job site using RTDs and thermocouples, *ISA Transactions*, **Volume 33(3)**, pp 287-292.

Royston P.,1992, Approximating the Shapiro-Wilk W-test for non-normality, *Statistics and Computing*, Springer, **Volume 2**, Issue 3, pp 117-119.

Rubinstein, J.,1986, Effective equations for flow in random porous media with a large number of scales. *Journal of Fluid Mechanics*, **Volume 170**: pp 379-383.

Sadegh, A., Jiji L. and Weinbaum, S., 1987, Boundary integral equation technique with application to freezing around a buried pipe, *International Journal of Heat and Mass Transfer*, **Volume 30**: Issue 2, pp 223-232.

Schneider, P.J., 1973, Handbook of Heat Transfer, *McGraw-Hill USA*, Section 3: Conduction (1<sup>st</sup> edition).

Tarnawski, V. R., McCombie, M. L., Momose, T., Sakaguchi, I., & Leong, W. H., 2013, Thermal Conductivity of Standard Sands. Part III. Full Range of Saturation, *International Journal of Thermophysics*, **Volume 34(6)**: pp 1130-1147.

Thiyagarajan, R., & Yovanovich, M. M., 1974, Thermal resistance of a buried cylinder with constant flux boundary condition., *Journal of Heat Transfer*, **Volume 96(2)**: pp 249-250

Wentworth, Chester K., 1922, A scale of grade and class terms for clastic sediments, *The Journal of Geology*, **Volume 30(5)**: pp 377-392.

Wintehkorn, H.F., 1960, Behaviour of Moist Soils in a Thermal Energy Field, *Proceedings of the 9th National Conference on Clay & Clay Minerals*, NAS-NRC, **Volume 9**: pp 85-103.

Zakarian, E., Holbeach, J., & Morgan, J. E. P. (2012, April). A holistic approach to steady-state heat transfer from partially and fully buried pipelines. In *Offshore Technology Conference*. Offshore Technology Conference.

Zhang, Z. F., 2014, Relationship between Anisotropy in Soil Hydraulic Conductivity and Saturation, *Vadose Zone Journal*, **Volume 13(6)**.

# Appendix A- Benchmark Tests Results

## Benchmark Tests

Heater Length, L= 850.9 mm

Dry Test 1:

| Burial<br>Depth<br>Ratio<br>(D/d) | $T_{\text{heater}}$ | $T_{\text{boundary}}$ | $\Delta T$ | $P_{\text{total}}$<br>(Experimental) | $P_{\text{unit-length}}$<br>(Experimental) | $P_{\text{unit-length}}$<br>(Analytical) | Difference | Experimental<br>Shape Factor | Experimental<br>Average<br>Shape Factor | Analytical<br>Shape<br>Factor,<br>T=C | Analytical<br>Shape<br>Factor,<br>q=C |
|-----------------------------------|---------------------|-----------------------|------------|--------------------------------------|--------------------------------------------|------------------------------------------|------------|------------------------------|-----------------------------------------|---------------------------------------|---------------------------------------|
|                                   | °C                  | °C                    | °C         | W                                    | (W/m)                                      | (W/m)                                    |            |                              |                                         |                                       |                                       |
| 0.8                               | 23.41               | 0.87                  | 22.54      | 16.023                               | 18.83                                      | 20.8                                     | -9.5       | 3.54                         |                                         |                                       |                                       |
|                                   | 32.81               | 1.07                  | 31.74      | 22.869                               | 26.88                                      | 29.2                                     | -8.0       | 3.59                         |                                         |                                       |                                       |
|                                   | 42.18               | 1.39                  | 40.79      | 28.6                                 | 33.61                                      | 37.6                                     | -10.6      | 3.49                         |                                         |                                       |                                       |
|                                   | 51.55               | 1.68                  | 49.87      | 35.41                                | 41.61                                      | 45.9                                     | -9.3       | 3.54                         |                                         |                                       |                                       |
|                                   | 61.03               | 2.04                  | 58.99      | 42.693                               | 50.17                                      | 54.3                                     | -7.6       | 3.60                         |                                         |                                       |                                       |
|                                   | 65.69               | 2.22                  | 63.47      | 45.57                                | 53.56                                      | 58.5                                     | -8.5       | 3.58                         | 3.58                                    | 3.90                                  | 3.73                                  |
|                                   | 60.71               | 2.16                  | 58.55      | 44.65                                | 52.47                                      | 53.9                                     | -2.6       | 3.80                         |                                         |                                       |                                       |
|                                   | 52.85               | 1.83                  | 51.02      | 35.7                                 | 41.96                                      | 47                                       | -10.7      | 3.48                         |                                         |                                       |                                       |
|                                   | 41.79               | 1.34                  | 40.45      | 28.98                                | 34.06                                      | 37.3                                     | -8.7       | 3.57                         |                                         |                                       |                                       |
|                                   | 32.49               | 1.04                  | 31.45      | 23.1                                 | 27.15                                      | 29                                       | -6.4       | 3.66                         |                                         |                                       |                                       |
|                                   | 23.21               | 0.72                  | 22.49      | 16.17                                | 19.00                                      | 20.7                                     | -8.2       | 3.58                         |                                         |                                       |                                       |

Dry Test 2:

| Burial<br>Depth<br>Ratio<br>(D/d) | $T_{\text{heater}}$ | $T_{\text{boundary}}$ | $\Delta T$ | $P_{\text{total}}$<br>(Experimental) | $P_{\text{unit-length}}$<br>(Experimental) | $P_{\text{unit-length}}$<br>(Analytical) | Difference | Experimental<br>Shape Factor | Experimental<br>Average<br>Shape Factor | Analytical<br>Shape<br>Factor,<br>T=C | Analytical<br>Shape<br>Factor,<br>q=C |
|-----------------------------------|---------------------|-----------------------|------------|--------------------------------------|--------------------------------------------|------------------------------------------|------------|------------------------------|-----------------------------------------|---------------------------------------|---------------------------------------|
|                                   | °C                  | °C                    | °C         | W                                    | (W/m)                                      | (W/m)                                    | %          |                              |                                         |                                       |                                       |
| 1.91                              | 22.81               | 1.89                  | 20.92      | 12.00                                | 14.10                                      | 13.80                                    | 2.15       | 2.86                         |                                         |                                       |                                       |
|                                   | 32.34               | -0.02                 | 32.36      | 16.95                                | 19.92                                      | 21.30                                    | -6.49      | 2.61                         |                                         |                                       |                                       |
|                                   | 41.85               | 0.01                  | 41.84      | 21.72                                | 25.52                                      | 27.50                                    | -7.20      | 2.58                         |                                         |                                       |                                       |
|                                   | 51.38               | 0.16                  | 51.22      | 27.25                                | 32.02                                      | 33.70                                    | -4.98      | 2.65                         |                                         |                                       |                                       |
|                                   | 60.70               | 0.29                  | 60.41      | 32.97                                | 38.74                                      | 39.70                                    | -2.41      | 2.72                         |                                         |                                       |                                       |
|                                   | 64.12               | 0.89                  | 63.23      | 34.36                                | 40.38                                      | 41.60                                    | -2.94      | 2.71                         | 2.66                                    | 2.79                                  | 2.76                                  |
|                                   | 60.52               | 0.92                  | 59.60      | 31.32                                | 36.81                                      | 39.20                                    | -6.10      | 2.62                         |                                         |                                       |                                       |
|                                   | 51.32               | 1.19                  | 50.13      | 27.14                                | 31.90                                      | 33.00                                    | -3.33      | 2.70                         |                                         |                                       |                                       |
|                                   | 41.85               | 1.01                  | 40.84      | 21.30                                | 25.03                                      | 26.90                                    | -6.95      | 2.60                         |                                         |                                       |                                       |
|                                   | 32.44               | 0.47                  | 31.97      | 17.12                                | 20.12                                      | 21.00                                    | -4.18      | 2.67                         |                                         |                                       |                                       |
|                                   | 23.04               | 0.31                  | 22.73      | 11.69                                | 13.74                                      | 14.90                                    | -7.77      | 2.56                         |                                         |                                       |                                       |

Dry Test 3:

| Burial<br>Depth<br>Ratio<br>(D/d) | $T_{\text{heater}}$ | $T_{\text{boundary}}$ | $\Delta T$ | $P_{\text{total}}$<br>(Experimental) | $P_{\text{unit-length}}$<br>(Experimental) | $P_{\text{unit-length}}$<br>(Analytical) | Difference | Experimental<br>Shape Factor | Experimental<br>Average<br>Shape Factor | Analytical<br>Shape<br>Factor,<br>T=C | Analytical<br>Shape<br>Factor,<br>q=C |
|-----------------------------------|---------------------|-----------------------|------------|--------------------------------------|--------------------------------------------|------------------------------------------|------------|------------------------------|-----------------------------------------|---------------------------------------|---------------------------------------|
|                                   | °C                  | °C                    | °C         | W                                    | (W/m)                                      | (W/m)                                    | %          |                              |                                         |                                       |                                       |
| 2.86                              | 23.39               | -0.23                 | 23.62      | 10.84                                | 12.74                                      | 13.50                                    | -5.63      | 2.29                         |                                         |                                       |                                       |
|                                   | 32.92               | -0.12                 | 33.04      | 15.35                                | 18.04                                      | 18.90                                    | -4.55      | 2.31                         |                                         |                                       |                                       |
|                                   | 42.32               | 0.10                  | 42.22      | 20.13                                | 23.66                                      | 24.10                                    | -1.84      | 2.37                         |                                         |                                       |                                       |
|                                   | 51.59               | 1.59                  | 50.00      | 24.20                                | 28.44                                      | 28.60                                    | -0.56      | 2.41                         |                                         |                                       |                                       |
|                                   | 61.30               | -0.05                 | 61.35      | 28.57                                | 33.58                                      | 35.10                                    | -4.34      | 2.32                         |                                         |                                       |                                       |
|                                   | 70.71               | 0.48                  | 70.23      | 33.33                                | 39.17                                      | 40.20                                    | -2.56      | 2.36                         |                                         |                                       |                                       |
|                                   | 75.39               | 2.10                  | 73.29      | 34.62                                | 40.69                                      | 41.90                                    | -2.90      | 2.35                         | 2.33                                    | 2.42                                  | 2.41                                  |
|                                   | 70.77               | 0.08                  | 70.69      | 33.00                                | 38.78                                      | 40.40                                    | -4.00      | 2.32                         |                                         |                                       |                                       |
|                                   | 61.23               | 0.01                  | 61.22      | 28.33                                | 33.29                                      | 35.00                                    | -4.87      | 2.30                         |                                         |                                       |                                       |
|                                   | 51.53               | 1.88                  | 49.65      | 23.27                                | 27.35                                      | 28.40                                    | -3.71      | 2.33                         |                                         |                                       |                                       |
|                                   | 42.33               | -0.03                 | 42.36      | 19.61                                | 23.05                                      | 24.20                                    | -4.77      | 2.31                         |                                         |                                       |                                       |
|                                   | 32.83               | -0.12                 | 32.95      | 14.98                                | 17.60                                      | 18.80                                    | -6.36      | 2.26                         |                                         |                                       |                                       |
|                                   | 23.32               | 0.00                  | 23.32      | 10.76                                | 12.65                                      | 13.30                                    | -4.92      | 2.30                         |                                         |                                       |                                       |

Dry Test 4:

| Burial<br>Depth<br>Ratio<br>(D/d) | $T_{\text{heater}}$ | $T_{\text{boundary}}$ | $\Delta T$ | $P_{\text{total}}$<br>(Experimental) | $P_{\text{unit-length}}$<br>(Experimental) | $P_{\text{unit-length}}$<br>(Analytical) | Difference | Experimental<br>Shape Factor | Experimental<br>Average<br>Shape Factor | Analytical<br>Shape<br>Factor,<br>T=C | Analytical<br>Shape<br>Factor,<br>q=C |
|-----------------------------------|---------------------|-----------------------|------------|--------------------------------------|--------------------------------------------|------------------------------------------|------------|------------------------------|-----------------------------------------|---------------------------------------|---------------------------------------|
|                                   | °C                  | °C                    | °C         | W                                    | (W/m)                                      | (W/m)                                    | %          |                              |                                         |                                       |                                       |
|                                   | 22.98               | -0.04                 | 23.02      | 8.90                                 | 10.45                                      | 11.10                                    | -5.82      | 1.92                         |                                         |                                       |                                       |
|                                   | 32.43               | 0.01                  | 32.42      | 12.42                                | 14.60                                      | 15.60                                    | -6.41      | 1.91                         |                                         |                                       |                                       |
|                                   | 41.85               | 0.07                  | 41.78      | 16.99                                | 19.97                                      | 20.10                                    | -0.66      | 2.03                         |                                         |                                       |                                       |
|                                   | 51.16               | 0.48                  | 50.68      | 20.40                                | 23.97                                      | 24.30                                    | -1.34      | 2.00                         |                                         |                                       |                                       |
|                                   | 60.56               | 0.18                  | 60.38      | 24.41                                | 28.69                                      | 29.00                                    | -1.08      | 2.01                         |                                         |                                       |                                       |
|                                   | 69.71               | 0.65                  | 69.06      | 27.74                                | 32.60                                      | 33.20                                    | -1.80      | 2.00                         |                                         |                                       |                                       |
| 5                                 | 79.44               | 1.08                  | 78.36      | 30.75                                | 36.14                                      | 37.60                                    | -3.89      | 1.95                         | 1.95                                    | 2.03                                  | 2.03                                  |
|                                   | 69.77               | 0.71                  | 69.06      | 27.77                                | 32.64                                      | 33.20                                    | -1.70      | 2.00                         |                                         |                                       |                                       |
|                                   | 60.50               | 0.39                  | 60.11      | 23.25                                | 27.32                                      | 28.90                                    | -5.45      | 1.93                         |                                         |                                       |                                       |
|                                   | 51.06               | 0.21                  | 50.85      | 19.87                                | 23.35                                      | 24.40                                    | -4.30      | 1.95                         |                                         |                                       |                                       |
|                                   | 41.52               | 0.14                  | 41.38      | 15.86                                | 18.64                                      | 19.90                                    | -6.34      | 1.91                         |                                         |                                       |                                       |
|                                   | 32.25               | 0.02                  | 32.23      | 12.32                                | 14.48                                      | 15.50                                    | -6.59      | 1.90                         |                                         |                                       |                                       |
|                                   | 22.87               | -0.02                 | 22.88      | 8.72                                 | 10.25                                      | 11.00                                    | -6.84      | 1.90                         |                                         |                                       |                                       |

# Calibration of RTDs

| Serial           | RTD number | Offset | Set Temperature (°C) |       |         |         |
|------------------|------------|--------|----------------------|-------|---------|---------|
|                  |            |        | 80                   | 40    | 5       | -5      |
| 1                | 22         | 1.78   | 80                   | 39.97 | 4.98    | -5.06   |
| 2                | 33         | 1.65   | 80.16                | 40.11 | 5.098   | -4.905  |
| 3                | 32         | 1.76   | 80.08                | 40.05 | 5.067   | -4.932  |
| 4                | 29         | 1.89   | 80.06                | 39.89 | 5.052   | -4.945  |
| 5                | 39         | 1.86   | 79.76                | 39.87 | 4.985   | -4.972  |
| 6                | 37         | 1.84   | 79.85                | 39.88 | 5.006   | -4.972  |
| 7                | 15         | 1.78   | 80.18                | 40.07 | 5.13    | -4.842  |
| 8                | 42         | 1.91   | 80.16                | 40.04 | 5.03    | -4.97   |
| 9                | 4          | 1.94   | 80.17                | 39.98 | 4.97    | -5.02   |
| 10               | 25         | 1.95   | 80.05                | 39.97 | 5.01    | -4.972  |
| 11               | 36         | 1.7    | 79.71                | 39.83 | 5.145   | -4.725  |
| 12               | 30         | 1.97   | 79.91                | 39.89 | 5.01    | -4.935  |
| 13               | 35         | 1.81   | 80.15                | 40.08 | 5.055   | -4.945  |
| 14               | 31         | 1.81   | 80.01                | 39.96 | 5.002   | -4.975  |
| 15               | 23         | 1.74   | 80.08                | 40.04 | 5.04    | -4.945  |
| 16               | 1          | 1.84   | 79.87                | 39.88 | 4.995   | -4.94   |
| 17               | 18         | 1.77   | 79.91                | 39.93 | 5.005   | -4.96   |
| 18               | 38         | 1.76   | 80.07                | 39.99 | 5.043   | -4.92   |
| 19               | 41         | 1.74   | 80.09                | 40.05 | 5.07    | -4.935  |
| 20               | 3          | 1.95   | 80.08                | 40.01 | 5.01    | -4.98   |
| 21               | 27         | 1.79   | 79.98                | 40    | 5.075   | -4.897  |
| 22               | 21         | 1.73   | 79.98                | 39.98 | 5.035   | -4.95   |
| 23               | 40         | 1.74   | 79.97                | 39.97 | 5.033   | -4.95   |
| 24               | 26         | 1.76   | 80.02                | 40    | 5.042   | -4.94   |
| 25               | 34         | 1.75   | 80.01                | 39.97 | 4.995   | -5.01   |
| 26               | 45         | 1.96   | 80.05                | 39.98 | 4.985   | -5.02   |
| 27               | 13         | 1.96   | 80.12                | 40.06 | 5.07    | -4.935  |
| 28               | 20         | 1.79   | 79.9                 | 39.92 | 5.04    | -4.92   |
| 29               | 28         | 1.77   | 79.92                | 39.88 | 4.981   | -4.98   |
| 30               | 19         | 1.68   | 80.09                | 40.05 | 5.03    | -4.97   |
| 31               | 34         | 1.75   | 80.18                | 40.08 | 5.084   | -4.9    |
| Average          |            |        | 80.02                | 39.98 | 5.03    | -4.95   |
| Percentage Error |            |        | 0.02298              | -0.05 | 0.69226 | -1.0826 |

# Uncertainty Analysis

Dry Test 1:

| $P_{\text{unit-length}}$<br>(Experimental) | Shape Factor<br>(Experimental) |       |       |       |      |       |       |       |       |         |
|--------------------------------------------|--------------------------------|-------|-------|-------|------|-------|-------|-------|-------|---------|
| (W/m)                                      |                                | $a_q$ | $a_t$ | $a_k$ | $k$  | $w_q$ | $w_t$ | $w_k$ | $w_s$ | % $w_s$ |
| 18.83                                      | 3.54                           | 1     | -1    | -1    | 0.24 | 1.88  | 0.01  | 0.02  | 0.50  | 14.14   |
| 26.88                                      | 3.59                           | 1     | -1    | -1    | 0.24 | 2.69  | 0.01  | 0.02  | 0.51  | 14.14   |
| 33.61                                      | 3.49                           | 1     | -1    | -1    | 0.24 | 3.36  | 0.01  | 0.02  | 0.49  | 14.14   |
| 41.61                                      | 3.54                           | 1     | -1    | -1    | 0.24 | 4.16  | 0.01  | 0.02  | 0.50  | 14.14   |
| 50.17                                      | 3.60                           | 1     | -1    | -1    | 0.24 | 5.02  | 0.01  | 0.02  | 0.51  | 14.14   |
| 53.56                                      | 3.58                           | 1     | -1    | -1    | 0.24 | 5.36  | 0.01  | 0.02  | 0.51  | 14.14   |
| 52.47                                      | 3.80                           | 1     | -1    | -1    | 0.24 | 5.25  | 0.01  | 0.02  | 0.54  | 14.14   |
| 41.96                                      | 3.48                           | 1     | -1    | -1    | 0.24 | 4.20  | 0.01  | 0.02  | 0.49  | 14.14   |
| 34.06                                      | 3.57                           | 1     | -1    | -1    | 0.24 | 3.41  | 0.01  | 0.02  | 0.50  | 14.14   |
| 27.15                                      | 3.66                           | 1     | -1    | -1    | 0.24 | 2.71  | 0.01  | 0.02  | 0.52  | 14.14   |
| 19.00                                      | 3.58                           | 1     | -1    | -1    | 0.24 | 1.90  | 0.01  | 0.02  | 0.51  | 14.14   |

Dry Test 2:

| $P_{\text{unit-length}}$<br>(Experimental) | Shape Factor<br>(Experimental) |       |       |       |      |       |       |       |       |         |
|--------------------------------------------|--------------------------------|-------|-------|-------|------|-------|-------|-------|-------|---------|
| (W/m)                                      |                                | $a_q$ | $a_t$ | $a_k$ | $k$  | $w_q$ | $w_t$ | $w_k$ | $w_s$ | % $w_s$ |
| 14.10                                      | 2.86                           | 1     | -1    | -1    | 0.24 | 1.41  | 0.01  | 0.02  | 0.40  | 14.14   |
| 19.92                                      | 2.61                           | 1     | -1    | -1    | 0.24 | 1.99  | 0.01  | 0.02  | 0.37  | 14.14   |
| 25.52                                      | 2.58                           | 1     | -1    | -1    | 0.24 | 2.55  | 0.01  | 0.02  | 0.37  | 14.14   |
| 32.02                                      | 2.65                           | 1     | -1    | -1    | 0.24 | 3.20  | 0.01  | 0.02  | 0.37  | 14.14   |
| 38.74                                      | 2.72                           | 1     | -1    | -1    | 0.24 | 3.87  | 0.01  | 0.02  | 0.38  | 14.14   |
| 40.38                                      | 2.71                           | 1     | -1    | -1    | 0.24 | 4.04  | 0.01  | 0.02  | 0.38  | 14.14   |
| 36.81                                      | 2.62                           | 1     | -1    | -1    | 0.24 | 3.68  | 0.01  | 0.02  | 0.37  | 14.14   |
| 31.90                                      | 2.70                           | 1     | -1    | -1    | 0.24 | 3.19  | 0.01  | 0.02  | 0.38  | 14.14   |
| 25.03                                      | 2.60                           | 1     | -1    | -1    | 0.24 | 2.50  | 0.01  | 0.02  | 0.37  | 14.14   |
| 20.12                                      | 2.67                           | 1     | -1    | -1    | 0.24 | 2.01  | 0.01  | 0.02  | 0.38  | 14.14   |
| 13.74                                      | 2.56                           | 1     | -1    | -1    | 0.24 | 1.37  | 0.01  | 0.02  | 0.36  | 14.14   |

Dry Test 3:

| $P_{\text{unit-length}}$<br>(Experimental)<br>(W/m) | Shape Factor<br>(Experimental) | $a_q$ | $a_t$ | $a_k$ | $k$  | $w_q$ | $w_t$ | $w_k$ | $w_s$ | % $w_s$ |
|-----------------------------------------------------|--------------------------------|-------|-------|-------|------|-------|-------|-------|-------|---------|
| 12.74                                               | 2.29                           | 1     | -1    | -1    | 0.24 | 1.27  | 0.01  | 0.02  | 0.32  | 14.14   |
| 18.04                                               | 2.31                           | 1     | -1    | -1    | 0.24 | 1.80  | 0.01  | 0.02  | 0.33  | 14.14   |
| 23.66                                               | 2.37                           | 1     | -1    | -1    | 0.24 | 2.37  | 0.01  | 0.02  | 0.34  | 14.14   |
| 28.44                                               | 2.41                           | 1     | -1    | -1    | 0.24 | 2.84  | 0.01  | 0.02  | 0.34  | 14.14   |
| 33.58                                               | 2.32                           | 1     | -1    | -1    | 0.24 | 3.36  | 0.01  | 0.02  | 0.33  | 14.14   |
| 39.17                                               | 2.36                           | 1     | -1    | -1    | 0.24 | 3.92  | 0.01  | 0.02  | 0.33  | 14.14   |
| 40.69                                               | 2.35                           | 1     | -1    | -1    | 0.24 | 4.07  | 0.01  | 0.02  | 0.33  | 14.14   |
| 38.78                                               | 2.32                           | 1     | -1    | -1    | 0.24 | 3.88  | 0.01  | 0.02  | 0.33  | 14.14   |
| 33.29                                               | 2.30                           | 1     | -1    | -1    | 0.24 | 3.33  | 0.01  | 0.02  | 0.33  | 14.14   |
| 27.35                                               | 2.33                           | 1     | -1    | -1    | 0.24 | 2.73  | 0.01  | 0.02  | 0.33  | 14.14   |
| 23.05                                               | 2.31                           | 1     | -1    | -1    | 0.24 | 2.30  | 0.01  | 0.02  | 0.33  | 14.14   |
| 17.60                                               | 2.26                           | 1     | -1    | -1    | 0.24 | 1.76  | 0.01  | 0.02  | 0.32  | 14.14   |
| 12.65                                               | 2.30                           | 1     | -1    | -1    | 0.24 | 1.26  | 0.01  | 0.02  | 0.32  | 14.14   |

Dry Test 4:

| $P_{\text{unit-length}}$<br>(Experimental) | Shape Factor<br>(Experimental) | $a_q$ | $a_t$ | $a_k$ | $k$  | $w_q$ | $w_t$ | $w_k$ | $w_s$ | % $w_s$ |
|--------------------------------------------|--------------------------------|-------|-------|-------|------|-------|-------|-------|-------|---------|
| 10.45                                      | 1.92                           | 1     | -1    | -1    | 0.24 | 1.05  | 0.01  | 0.02  | 0.27  | 14.14   |
| 14.60                                      | 1.91                           | 1     | -1    | -1    | 0.24 | 1.46  | 0.01  | 0.02  | 0.27  | 14.14   |
| 19.97                                      | 2.03                           | 1     | -1    | -1    | 0.24 | 2.00  | 0.01  | 0.02  | 0.29  | 14.14   |
| 23.97                                      | 2.00                           | 1     | -1    | -1    | 0.24 | 2.40  | 0.01  | 0.02  | 0.28  | 14.14   |
| 28.69                                      | 2.01                           | 1     | -1    | -1    | 0.24 | 2.87  | 0.01  | 0.02  | 0.28  | 14.14   |
| 32.60                                      | 2.00                           | 1     | -1    | -1    | 0.24 | 3.26  | 0.01  | 0.02  | 0.28  | 14.14   |
| 36.14                                      | 1.95                           | 1     | -1    | -1    | 0.24 | 3.61  | 0.01  | 0.02  | 0.28  | 14.14   |
| 32.64                                      | 2.00                           | 1     | -1    | -1    | 0.24 | 3.26  | 0.01  | 0.02  | 0.28  | 14.14   |
| 27.32                                      | 1.93                           | 1     | -1    | -1    | 0.24 | 2.73  | 0.01  | 0.02  | 0.27  | 14.14   |
| 23.35                                      | 1.95                           | 1     | -1    | -1    | 0.24 | 2.34  | 0.01  | 0.02  | 0.28  | 14.14   |
| 18.64                                      | 1.91                           | 1     | -1    | -1    | 0.24 | 1.86  | 0.01  | 0.02  | 0.27  | 14.14   |
| 14.48                                      | 1.90                           | 1     | -1    | -1    | 0.24 | 1.45  | 0.01  | 0.02  | 0.27  | 14.14   |
| 10.25                                      | 1.90                           | 1     | -1    | -1    | 0.24 | 1.02  | 0.01  | 0.02  | 0.27  | 14.14   |

# Appendix B- Saturated Tests Results

## Sample Saturated Test

|                                                   |          |
|---------------------------------------------------|----------|
| Dry Conductivity (W/m-K)                          | 0.23     |
| Density of Dry Sand (kg-m <sup>3</sup> )          | 1563.60  |
| Mass of container with fittings (kg)              | 0.67     |
| Mass of container with dry sand (kg)              | 6.93     |
| Mass of Dry sand (kg)                             | 6.26     |
| Mass of valve with hose (kg)                      | 0.19     |
| Mass of container with wet sand (kg)              | 8.82     |
| Mass of container with fittings and water (kg)    | 1.16     |
| Water trapped in fittings (kg)                    | 0.49     |
| Mass of wet sand (kg)                             | 7.48     |
| Mass of water content (kg)                        | 1.22     |
| Porosity, n                                       | 0.41     |
| Volume of void, V <sub>v</sub> (m <sup>3</sup> )  | 0.001831 |
| Volume of Water, V <sub>w</sub> (m <sup>3</sup> ) | 0.001217 |
| So, Degree of saturation (S <sub>r</sub> )        | 0.665    |

## Properties of Saturated Sand

|                                                                    |         |
|--------------------------------------------------------------------|---------|
| Box weight with geo sheets, coarser sand, 18 RTDs (kg)             | 404.00  |
| Weight of the dry fine sand (kg)                                   | 274.00  |
| Volume of the soil box filled with dry fine sand (m <sup>3</sup> ) | 0.19    |
| Density of dry fine sand (kg/m <sup>3</sup> )                      | 1448.29 |
| Valve weight attached with the box (kg)                            | 0.37    |
| Perforated Sheet weight (kg)                                       | 2.6     |
| Washer and bolts weight (kg)                                       | 1.12    |
| Saturated sand weight with fittings (kg)                           | 784.00  |
| Water height excess from top of the box (cm)                       | 6.8     |
| Excess water volume (m <sup>3</sup> )                              | 0.051   |
| Excess water weight (kg)                                           | 50.85   |
| Saturated sand weight (kg)                                         | 325.80  |
| Water Content (kg)                                                 | 51.80   |
| $\rho_{\max}$                                                      | 1650.5  |
| $\rho_{\min}$                                                      | 1357.75 |
| Specific Gravity, G                                                | 2.66    |
| Water Density, $\rho_{\text{water}}$                               | 1000    |
| Void Ratio, e                                                      | 0.84    |
| $e_{\max}$                                                         | 0.96    |
| $e_{\min}$                                                         | 0.61    |
| Relative Density, $D_r$ (%)                                        | 35.25   |
| Porosity, n                                                        | 0.46    |
| Volume of void, $V_v$ (m <sup>3</sup> )                            | 0.086   |
| Volume of Water, $V_w$ (m <sup>3</sup> )                           | 0.052   |
| $S_o$ , Degree of saturation, $S_r$                                | 0.601   |

## Uniform Test

| Pipe Wall Temperature (°C) | Heater Current (A) | Power (W/m) |
|----------------------------|--------------------|-------------|
| 24.10                      | 0.69               | 97.20       |
| 33.48                      | 0.89               | 125.69      |
| 43.45                      | 1.20               | 169.65      |
| 53.11                      | 1.46               | 206.42      |
| 63.22                      | 1.69               | 239.12      |
| 66.78                      | 1.72               | 243.13      |
| 63.55                      | 1.64               | 231.17      |
| 53.62                      | 1.39               | 196.59      |
| 43.85                      | 1.14               | 160.84      |
| 33.89                      | 0.84               | 118.41      |
| 24.27                      | 0.65               | 91.85       |

## Open Trench Test

| Pipe Wall Temperature (°C) | Heater Current (A) | Power (W/m) |
|----------------------------|--------------------|-------------|
| 9.61                       | 0.38               | 53.12       |
| 13.83                      | 0.73               | 103.93      |
| 17.77                      | 1.23               | 173.01      |
| 21.61                      | 1.58               | 223.66      |
| 23.71                      | 1.71               | 240.70      |
| 21.83                      | 1.50               | 211.65      |

|       |      |        |
|-------|------|--------|
| 17.78 | 1.18 | 166.49 |
| 14.02 | 0.71 | 99.71  |
| 9.67  | 0.33 | 46.55  |

## Backfill Test 1

| Pipe Wall Temperature (°C) | Heater Current (A) | Power (W/m) |
|----------------------------|--------------------|-------------|
| 9.43                       | 0.20               | 28.65       |
| 19.07                      | 0.46               | 64.58       |
| 23.98                      | 0.55               | 77.62       |
| 28.69                      | 0.71               | 99.86       |
| 33.43                      | 0.80               | 112.85      |
| 38.13                      | 0.90               | 127.42      |
| 42.90                      | 1.05               | 148.65      |
| 47.91                      | 1.21               | 170.59      |
| 52.70                      | 1.30               | 183.28      |
| 62.42                      | 1.50               | 210.89      |
| 67.29                      | 1.58               | 222.59      |
| 72.12                      | 1.66               | 234.30      |
| 62.40                      | 1.43               | 201.63      |
| 52.64                      | 1.26               | 177.73      |
| 47.83                      | 1.11               | 156.85      |
| 42.79                      | 0.93               | 130.63      |
| 33.27                      | 0.71               | 100.61      |

|       |      |       |
|-------|------|-------|
| 23.74 | 0.46 | 64.77 |
| 14.24 | 0.27 | 37.86 |
| 9.50  | 0.16 | 22.93 |

## Backfill Test 2

| Pipe Wall Temperature (°C) | Heater Current (A) | Power (W/m) |
|----------------------------|--------------------|-------------|
| 9.11                       | 0.21               | 29.07       |
| 18.65                      | 0.45               | 63.47       |
| 23.69                      | 0.57               | 81.03       |
| 33.36                      | 0.83               | 117.64      |
| 38.14                      | 0.92               | 130.32      |
| 42.98                      | 1.11               | 157.21      |
| 52.83                      | 1.34               | 189.07      |
| 62.52                      | 1.54               | 217.71      |
| 72.76                      | 1.71               | 241.58      |
| 62.21                      | 1.44               | 202.88      |
| 52.51                      | 1.27               | 179.01      |
| 42.68                      | 0.96               | 135.52      |
| 37.86                      | 0.83               | 116.37      |
| 33.09                      | 0.73               | 102.25      |
| 23.63                      | 0.49               | 69.08       |
| 14.09                      | 0.26               | 36.00       |
| 9.31                       | 0.16               | 23.04       |

## Backfill Test 3

| Pipe Wall Temperature (°C) | Heater Current (A) | Power (W/m) |
|----------------------------|--------------------|-------------|
| 9.32                       | 0.31               | 43.92       |
| 18.76                      | 0.47               | 66.03       |
| 23.52                      | 0.65               | 91.04       |
| 33.29                      | 0.94               | 132.51      |
| 38.32                      | 1.08               | 152.14      |
| 42.97                      | 1.26               | 177.07      |
| 53.42                      | 1.51               | 212.26      |
| 63.22                      | 1.74               | 245.56      |
| 52.96                      | 1.41               | 198.30      |
| 42.42                      | 1.16               | 163.84      |
| 37.66                      | 0.99               | 140.19      |
| 32.87                      | 0.87               | 122.69      |
| 23.38                      | 0.66               | 93.25       |
| 13.92                      | 0.43               | 60.99       |
| 9.25                       | 0.29               | 41.48       |